INTERIM TECHNICAL REPORT #1 WAL REPORT #WAL 401-143-3

July 1, 1952 - May 1, 1953

Office of Ordnance Research

Contract #DA-19-020-ORD-1816

CORROSION AND PASSIVITY STUDIES WITH TITANIUM

by

H. E. Farnsworth and A. M. Russell

May, 1953

BARUS RESEARCH LABORATORY OF PHYSICS

Brown University

Providence 12, Rhode Island

This technical report has been prepared from a thesis submitted by Allan M. Russell in partial fulfillment of the requirements for the Degree of Master of Science in the Department of Physics in Brown University, entitled.

Low Energy Electron Diffraction from
a Single Crystal of Iodide Titanium.

The report was written by Allan M. Russell under the supervision of H. E. Farnsworth. The experimental work was performed by A. M. Russell and T. H. George, under the supervision of R. E. Schlier and H. E. Farnsworth. The photographs of the apparatus and the photomicrographs of the crystal were taken by Professor Carl W. Miller of the Department of Physics in Brown University.

INDEX OF MAJOR HEADINGS

ILLUSTRATIONS

INTRODUCTION

An Historical Introduction to Electron Diffraction In 1924 de Broglie introduced the hypothesis that the wave particle dualism, which had been applied to radiant energy in order to explain such experimental observations as the Compton effect and the photoelectric effect, could also be applied to particles such as electrons or molecules. Since a group of waves, under the influence of dispersion, interact to form a wave packet with a velocity far less than the velocity of the component wave, it was suggested that a wave packet be used to represent a particle moving with a velocity equal to the group velocity of the waves, which is the velocity of the wave packet.

Utilizing this hypothesis, but following the non-relativistic analysis due to Schrödinger[1], one may write

$$u' = u - \lambda \frac{\partial u}{\partial \lambda}, \tag{1}$$

where u' = group velocity, λ = wave length, u = wave velocity and

$$E = h\nu = \tfrac{1}{2}mv^2 + V(x,y,z), \tag{2}$$

where E = total energy of particle, h = Planck's constant, ν = frequency, m = particle mass, v = particle velocity and V = potential energy of particle. Substituting $u = \lambda\nu$ into (1) gives

$$u' = \lambda\nu - \lambda \frac{\partial}{\partial \lambda}(\lambda\nu) = \lambda\nu - \lambda\nu - \lambda^2 \frac{\partial \nu}{\partial \lambda} = -\lambda^2 \frac{\partial \nu}{\partial \lambda}. \tag{3}$$

The differentiation of (2) with respect to λ, holding x, y and z constant, yields

$$h \frac{\partial \nu}{\partial \lambda} = mv \frac{\partial v}{\partial \lambda}. \tag{4}$$

By combining (3) and (4) one obtains

$$u' = -\lambda^2 \frac{mv}{h} \frac{\partial v}{\partial \lambda} .$$

But from the hypothesis $u' = v$. The above equation may be written in the form

$$\frac{\partial v}{\partial \lambda} = -\frac{h}{m\lambda^2} . \qquad (5)$$

Integrating (5) and setting the constant of integration equal to zero one obtains

$$v = \frac{h}{m\lambda}, \qquad \text{or} \qquad p = \frac{h}{\lambda} . \qquad (6)$$

where p is the momentum of the particle.

Thus the de Broglie wave length associated with a particle is inversely proportional to the momentum of the particle with the constant of proportionality equal to Planck's constant.

If the wave character of particles was to be admitted it seemed reasonable to expect that wave properties such as diffraction and interference should also be exhibited by particles. It should be noted, however, that any diffraction "grating" would require a spacing of the order of atomic dimensions since the wave lengths involved are so small (for 100 volt electrons, $\lambda = 1.22\text{Å}$).

This difficulty, however, had been surmounted a decade earlier by Laue. When faced with the problem of diffracting X-rays, Laue used the regular arrangement of atoms in a crystal as a grating whose spacing was on the order of an angstrom. It is not surprising, therefore, that the first evidence of particle diffraction, obtained by Davisson and Germer in 1927, utilized essentially the same principle.

Davisson and Germer[2] directed a beam of low voltage electrons onto the face of a nickel crystal, and measured the intensity (number) of reflected electrons

as a function of the angle of reflection. They found that intensity peaks existed at certain angles of reflection and that the angular position of the peaks depended upon the orientation of the atoms in the crystal and the energy of the incident beam. This can be shown by utilizing the Bragg law for X-ray reflection:

$$N\lambda = d \sin \theta, \tag{7}$$

where N = order of reflection, λ = wave length of incident beam, d = spacing between atomic planes in the crystal and θ = angle of reflected beam. But for an electron which has been accelerated through a voltage V

$$p = mv = h\sqrt{\frac{2\ meV}{300}}$$

where m = mass of electron and e = charge on electron. Substituting this value of p into (6), and solving for λ, one obtains

$$\lambda = h\ \sqrt{\frac{150}{meV}}.$$

If λ is expressed in angstroms, this equation becomes

$$\lambda = \sqrt{\frac{150}{V}}. \tag{8}$$

The substitution of (8) into (7) and the consideration of only first order reflections (N = 1) yields

$$d \sin \theta = \sqrt{\frac{150}{V}}, \qquad \text{or} \qquad \theta = \sin^{-1} \frac{1}{d}\ \sqrt{\frac{150}{V}}. \tag{9}$$

The experiment of Davisson and Germer substantiates this result and, therefore, the original hypothesis of de Broglie.

Applications of Low-energy Electron Diffraction. Investigation has shown that low-energy (100 volts or less) electrons penetrate only a very short

distance into a metal crystal. It has, in fact, been concluded on the basis of experiment[3], that 90% of the reflected beam is due to the first two layers of atoms on the surface of a silver crystal. This differs markedly from the analogous situation for X-rays where the radiation penetrates far into the interior of a metal crystal. For this reason, one of the principle uses of low energy electron diffraction has been the study of the surface structure of metal single crystals.

The results obtained by Davisson and Germer in their original experiment[2] show that the position and intensity of diffraction maxima depend to a great extent upon the amount of adsorbed gas on the surface of the crystal. This is strikingly apparent when one considers that in order to obtain any diffraction beam at all the crystal must be heated for long periods of time in a vacuum so that the bulk of the adsorbed gas is removed.

This sensitivity to surface gas structure is precisely the characteristic that makes low energy electron diffraction techniques so valuable. Before extensive low energy diffraction studies had been made there was much doubt as to the very existence of an adsorbed gas structure. Many authorities held that the gas atoms were distributed in a random fashion over the surface

Earlier work in this laboratory[4] has confirmed the existence of definite preferred orientations for oxygen and nitrogen atoms on the surface of a copper single crystal.

Low energy electrons have been used also to investigate the structures of thin metal films evaporated onto the surface of a single crystal of the same or of a different metal[3]. In this way it is possible to determine the effect of the underlying crystal lattice on the arrangement of atoms in the film.

The Objectives of this Investigation

Titanium, the metal investigated in this experiment, is silvery-white in its pure form, has a strength comparable to iron, and is considerably lighter (Sp.G. = 4.5, as compared to 7.9 for iron and 2.7 for aluminum). It has a high melting point (1800°C, as compared to 1535°C for iron and 660°C for aluminum) and is corrosion resistant under average conditions.

It is believed that this passivity is intimately connected with the adsorption of gases on the surface of the metal. One of the ultimate aims of this investigation will be to examine the adsorption phenomena and attempt to correlate these with a passivity mechanism.

Before any controlled investigation of adsorption phenomena could be carried out, however, it was necessary to determine with what success the adsorbed gases could be removed, and to study the diffraction results obtained from the titanium crystal itself. This, therefore, was the first objective of this investigation.

THE TITANIUM CRYSTAL

The Hexagonal Close-Packed Structure

Before an analysis of the theoretical diffraction pattern can be made, a detailed knowledge of the crystal is required. Fortunately, this has already been achieved in the case of titanium. Reference to X-ray crystallographic data shows that titanium has two structures; alpha titanium which is hexagonal close-packed, and beta titanium which has a body-centered cubic structure. Since the transition from the alpha phase to the beta phase takes place at 850°C., only the alpha structure is considered in this investigation.

The hexagonal close-packed structure can be visualized most easily by considering the problem of packing many spheres of the same size into a large box so that as many spheres as possible can be accommodated. After the first layer has been placed, it will be apparent that each sphere has six nearest neighbors and that the whole array exhibits six-fold symmetry. As the second layer commences it will be clear that the same arrangement is being repeated, with each sphere resting directly above the space between three spheres in the lower level. When the disposition of the third layer is considered, there will be a choice between placing the spheres of the third layer directly over those in the first, or placing them not over those in the first layer. In either case the third layer will bear the same relation to the second that the second bears to the first. If the second choice is made the result will be a face centered cubic arrangement, but if the third layer is placed directly over the first, the spheres will be an hexagonal, close-packed array (see figure 2).

Since an arrangement of this kind exhibits six-fold symmetry it lends itself to representation in a non-orthogonal coordinate system with four axes. Such a representation is illustrated in figure 1. The set of atoms and bonds, symbolized by spheres and lines, corresponds to a unit cell of the crystal.

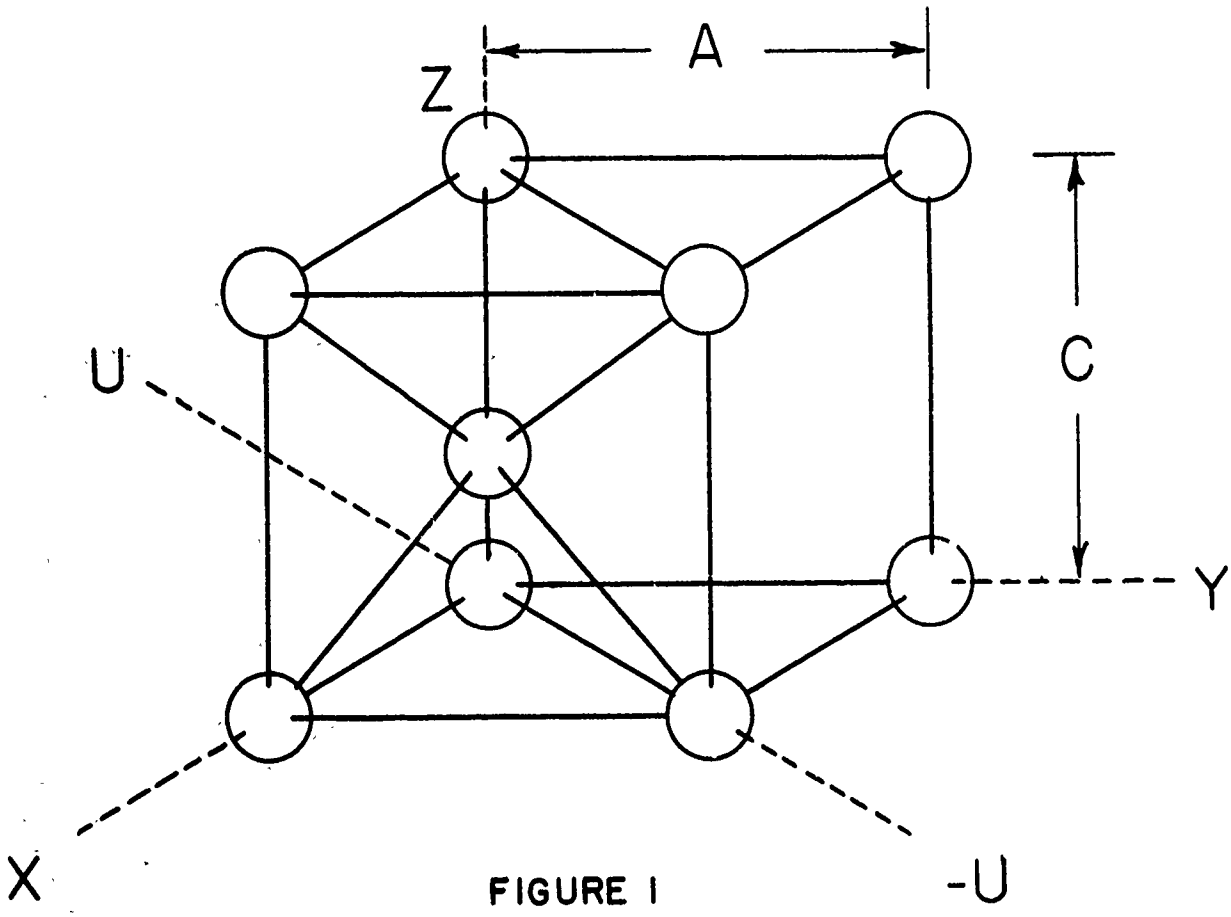

FIGURE 1

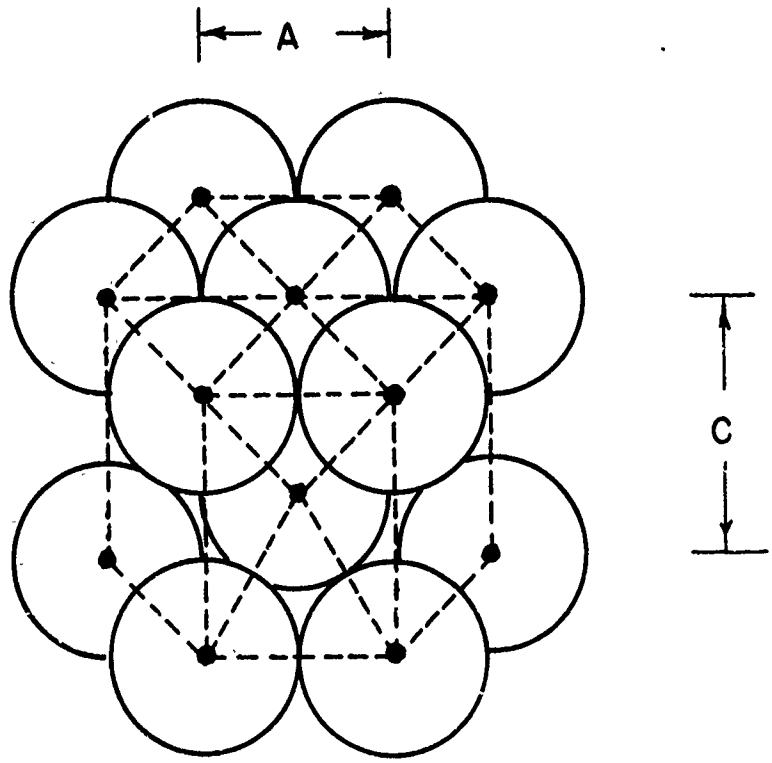

FIGURE 2

The index of a crystal plane is represented by the reciprocal of its intersection with each of the four axes (reduced, as usual to the four smallest integers having the same ratios). For example, the four spheres on the extreme right of figure 1 represent a plane whose indices, in the order (XYUZ), are (01$\bar{1}$0) The bar over the third index indicates that the plane crosses at a negative value of U. This system of indexing is called the Miller-Bravais system.

Physical Constants of the Titanium Crystal

The spacing between atoms of an hexagonal crystal is completely determined by two dimensions: A the distance between two adjacent atoms in the same plane, and B - the distance between odd planes (see figure 2). Crystallographic X ray data[5] gives the values for these constants as

$$A = 2.950 \text{ angstroms}, \qquad C = 4.683 \text{ angstroms}.$$

For the purpose of analyzing X-ray photographs used to orient the crystal, it is necessary to calculate the angles between planes for titanium. The only planes considered in the calculations were the ten most prominent, as listed for other hexagonal crystals[6]. The angle between two crystallographic planes may be expressed as follows[7].

$$\cos \phi = \frac{h_1h_2 + k_1k_2 + 1/2\,(h_1k_2 + h_2k_1) + \frac{3A^2}{4C^2}\, l_1l_2}{\sqrt{(h_1^2 + k_1^2 + h_1k_1 + \frac{3A^2}{4C^2}\, l_1^2)}\ \sqrt{(h_2^2 + k_2^2 + h_2k_2 + \frac{3A^2}{4C^2}\, l_2^2)}}.$$

The results of the calculations are given in table 1.

The Preparation of the Crystal

The titanium single crystal used in this investigation was obtained from the New Jersey Zinc Company through Watertown Arsenal. It was grown by the New Jersey Zinc Company using the strain-anneal method. This may be described briefly as follows An ingot

TABLE 1 ANGLES BETWEEN PLANES FOR ALPHA TITANIUM

(c.p. hexagonal)

(C/A 1.588)

	$10\bar{1}0$	0001	$10\bar{1}1$	$10\bar{1}2$	$11\bar{2}0$	$10\bar{1}3$	$11\bar{2}2$	$20\bar{2}1$	$10\bar{1}4$	$20\bar{2}3$
$10\bar{1}0$	00.0	90.0	28.8	47.5	30.0	58.6	42.8	14.8	65.4	39.2
	60.0		64.0	70.2	90.0	74.9	90.0	61.1	78.0	67.2
0001	00.0		61.4	41.5	90.0	31.5	57.6	74.7	24.8	50.7
$10\bar{1}1$	00.0		00.0	19.0	90.0	30.0	26.0	13.1	11.2	11.2
	52.2		49.5	76.1	40.6	50.5	67.2	44.7	64.3	50.2
	57.4		76.1			79.7	77.0	56.6	83.5	67.9
	81.0		86.8			87.2		72.8		87.9
$10\bar{1}2$			00.0	90.0	11.5	27.2	32.1	18.4	8.1	
			39.5	54.3	36.5	66.8	58.6	36.0	43.3	
			71.6		63.1	84.1	62.7	58.2	78.2	
			85.0		74.0		82.4	67.2	86.8	
$11\bar{2}0$				00.0	63.2	32.2	33.4	69.0	48.0	
				60.0	90.0	65.0	90.0	90.0	90.0	
$10\bar{1}3$					00.0	33.3	43.3	28.2	19.5	
					30.5	63.0	61.6	48.4	42.2	
					53.8	85.8	73.1	56.2	70.2	
					63.1		87.7	86.8	82.1	
$11\bar{2}2$						00.0	31.9	58.0	25.2	
						50.0	55.4	61.1	70.2	
						64.3	81.9	79.8	76.7	
						85.8				
$20\bar{2}1$							00.0	50.2	23.9	
							30.2	68.9	43.3	
							39.6	80.6	54.5	
							50.9	87.8	66.8	
$10\bar{1}4$								00.0	26.4	
								24.6	42.7	
								42.6	65.6	
								49.5	75.3	
$20\bar{1}3$									00.0	
									31.8	
									78.8	
									87.2	

of pure iodide titanium is cold-rolled to introduce strains into the bulk metal. It is sealed into a vial of fused quartz either in a vacuum or in an inert atmosphere, and the whole is heated to a temperature just above the transition temperature. It is then cycled above and below the transition temperature for many hours. This constant shifting of the atoms in the metal from one phase to the other tends to "jar" them into a preferred orientation determined by the strains in the metal.

After the crystal had been received by this laboratory it was mounted on an X-ray camera, and oriented by the Laue back-reflection method. In this method a thin pencil of 40,000 volt X-rays passes through a hole in a photographic film and strikes the surface of the crystal. The resultant reflected X-rays fall upon the photographic film. The selective reflection of the X rays from planes in the crystal creates reflected beams that register as spots on the photographic film, each spot corresponding to a particular crystal plane.

Figure 3 is a set of prints made from the X-ray negatives for this crystal. A is the initial photograph. The white dots correspond to the X ray beams, the spot in the center is due to the hole in the film through which the initial X-ray beam passes. After tentative calculations were made to approximate the orientation, the crystal was rotated, and negative B was exposed. It is apparent from the approximate two-fold symmetry that this exposure corresponds to the $01\bar{1}0$ plane, which is the side of the crystal as depicted in figure 2. In fact, the ratio of the distances between the four major spots on this negative is 1.58 and C/A for titanium is 1.588. The crystal was then rotated 90 degrees and exposure C was made. In this picture the spot for the 0001 plane (the ultimate objective) may be seen in the lower right hand corner. The crystal was once again rotated so as to bring this spot into the center of the film with the result shown in picture D. Note the six-fold symmetry corresponding to

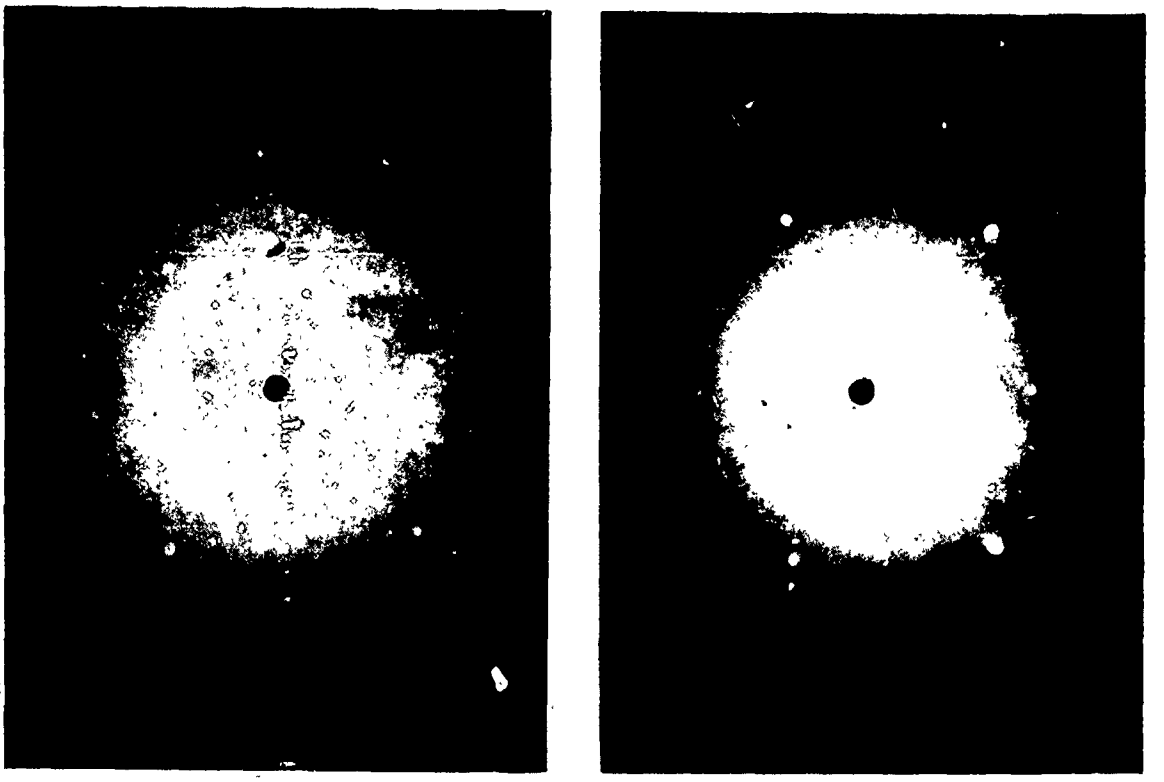

A B

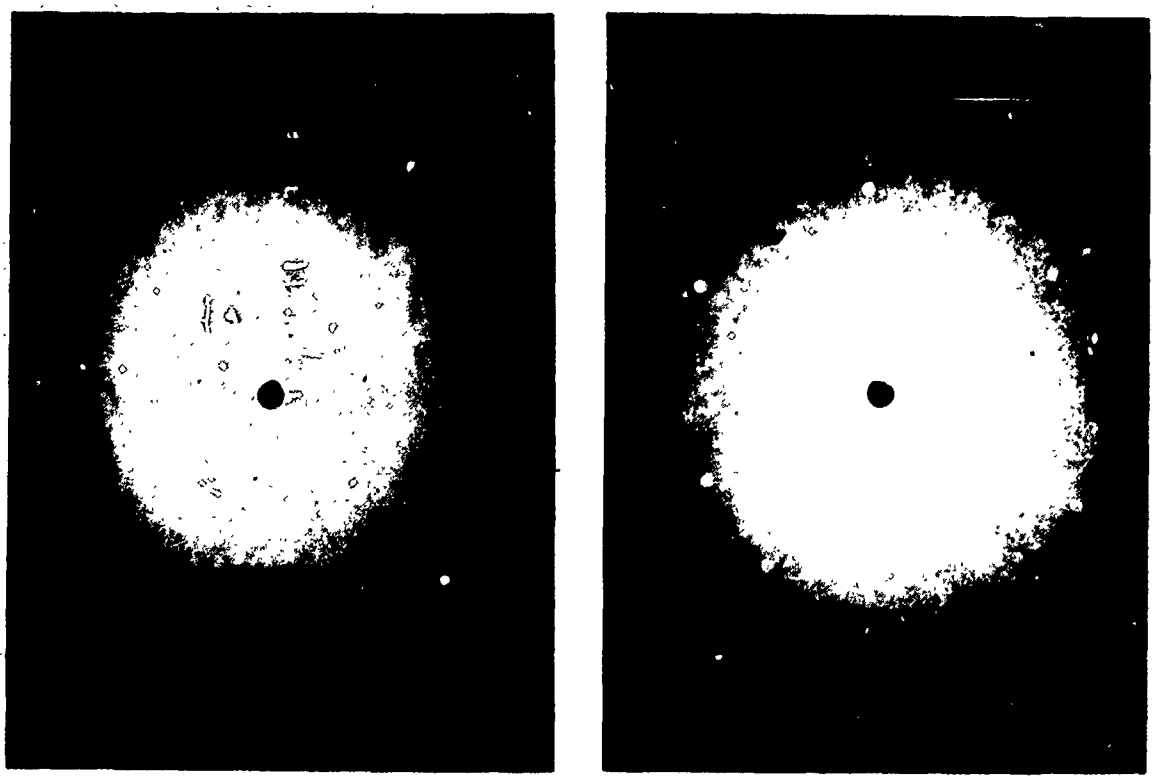

C D

FIGURE 3

the 0001 face or the top of the crystal as shown in figure 2.

The crystal, having once been oriented, was then cut parallel to the 0001 face with a high speed rubber-based wheel, provided by the A. P. DeSanno Company. Other cuts were also made to facilitate mounting the crystal. The face of the crystal was then prepared by grinding it on metallographic paper until the face showed no scratches deeper than those caused by #4/0 paper.

The appearance of the surface at this time can be seen in figure 4. These are photomicrographs taken of the crystal surface at a magnification of 1000x. Vertical illumination was used to bring out the character of the surface. The top exposure was of the crystal surface after it had been abraded with the 4/0 paper. That this gives a sufficiently smooth surface is apparent from the other two photomicrographs. The center exposure was taken after the crystal had been etched in 50% HF and 50% glycerin for approximately ten seconds. The bottom exposure corresponds to the results obtained from etching the crystal fifty seconds. The crystal was etched for a total of 120 seconds but no further improvement was detected. Note that the etch pits become larger as the crystal becomes flatter, indicating that the chemical action takes place along the surface much faster than into the bulk material.

The grooves on the crystal face which can be seen at the bottom of figure 4 correspond very well to the equilateral triangles which are characteristic of the 0001 face in the hexagonal structure (see figure 2). These lines, particularly at the upper right of the photomicrograph, correspond also to the six fold symmetry apparent from X-ray D, figure 3.

On the basis of the evidence described above it was concluded that the crystal was single, containing no detectable amounts of polycrystalline titanium.

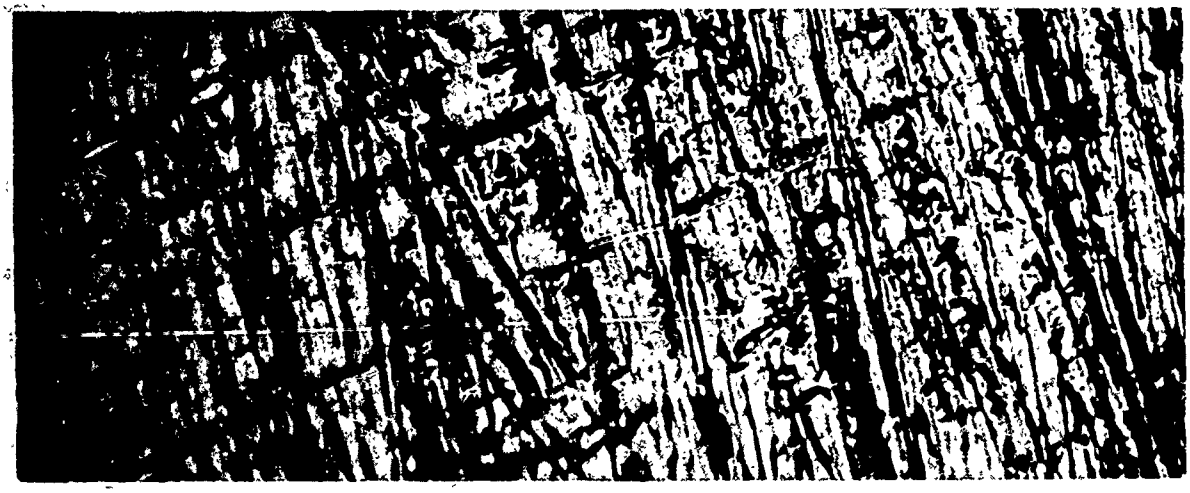

ABRADED SURFACE

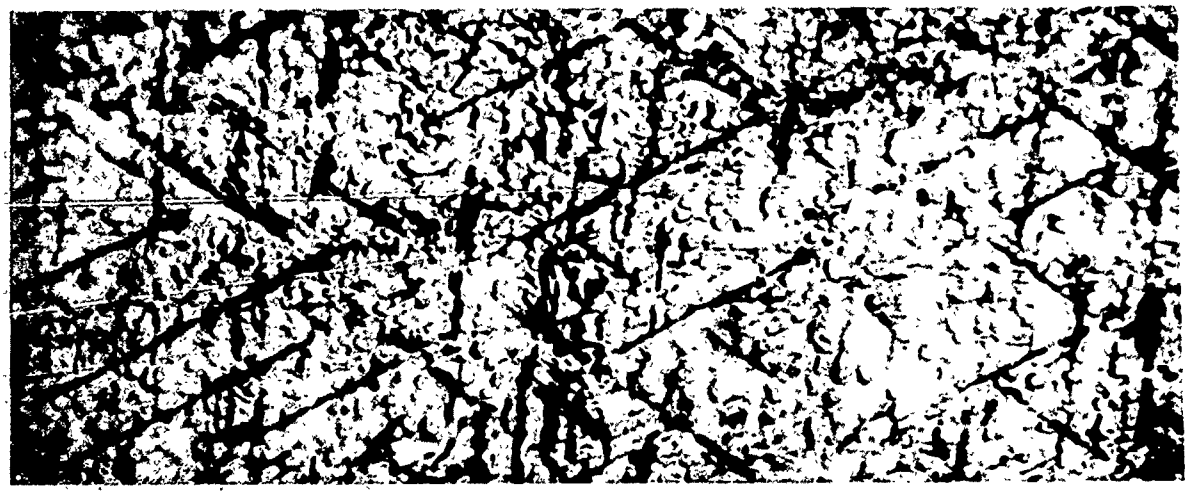

10 SECOND ETCH

50 SECOND ETCH

FIGURE 4 1000x

Furthermore, it was oriented in such a manner that the plane of the surface was parallel to the 0001 face. This face was the one used for the diffraction studies discussed here.

During the course of a diffraction experiment the crystal under investigation must be heated in vacuo, usually by electron bombardment. In the case of titanium this introduces two interesting problems.

In the first place, X-ray crystallographic data[5] shows that titanium undergoes a phase change somewhere between the temperatures of 850° 900°C. (Depending upon the amount of impurities present in the crystal). At the transition temperature the atoms in the crystal shift from a closely packed hexagonal structure to a body centered cubic array. It is necessary, therefore, to maintain outgassing temperatures below this transition value, as there is no guarantee that the crystal will return to exactly the same atomic configuration once it has undergone the transition. On the other hand, the amount of gas that can be removed from a metal crystal is dependent upon the temperature to which it can be heated. The problem, consequently, becomes one of heating the crystal as hot as possible, being certain, however, that the temperature never reaches 850°C.

The second problem evolves from the fact that titanium amalgamates with many other metals, some at rather low temperatures. It was necessary, therefore, to mount the crystal on a metal which has no eutectic with titanium below 900°C.

Fortunately, the solution to the second problem served as a solution to the first. It was found that molybdenum could be used for the crystal mounting as this metal satisfied the requirement mentioned above. It was also found that the molybdenum-titanium junction could be used as a thermocouple since the

thermoelectric potential varied from approximately 1 millivolt at 20° C. to 10 millivolts at 800° C. Figure 5 is a plot of the calibration of the titanium molybdenum thermocouple. It should be noted that the thermocouple could not be used above 850° C. as it behaved very erratically in the neighborhood of the transition temperature.

The crystal was mounted on a molybdenum block having approximately four times the bulk of the crystal itself. This, in turn was attached by means of a thin molybdenum shaft to a clamp which was wired to the end of a glass tube. The thin metal shaft prevented excessive heat conduction to the glass.

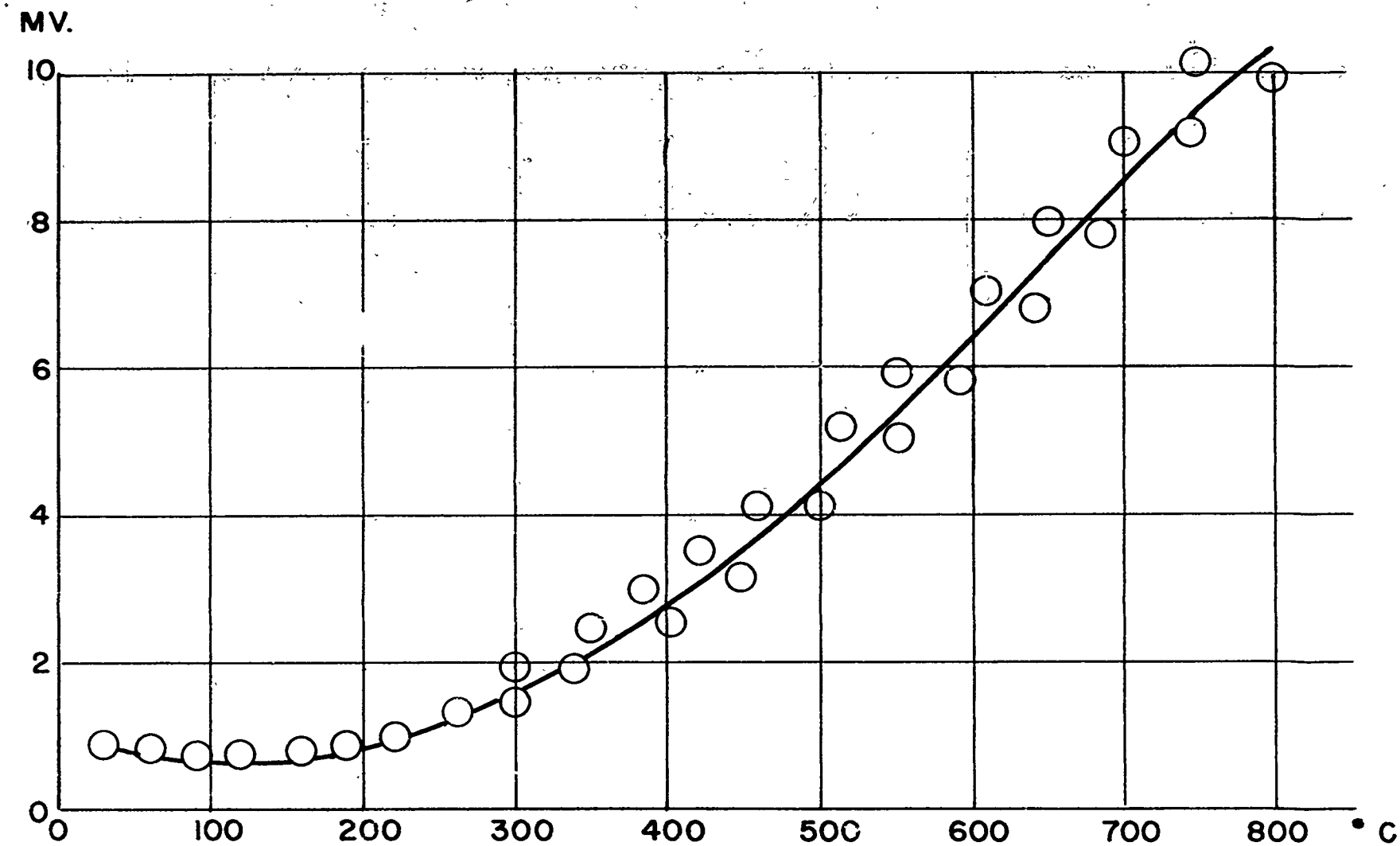

TITANIUM vs. MOLYBDENUM THERMOCOUPLE

FIGURE 5

CALCULATION OF ELECTRON DIFFRACTION BEAM

Theoretical Diffraction Beams from the 0001 Face Knowledge of the crystal form and the lattice constants of titanium makes possible the calculation of expected diffraction beams for the range of voltage to be used (in this case 0-250 volts) provided that the orientation of the crystal with respect to the incident beam is known.

The diffraction face is defined as a crystal plane perpendicular to the incident electron beam, and the diffraction azimuth as a crystal plane parallel to the plane which includes both the incident electron beam and the particular reflected electron beam considered. A little thought will show that if the face and azimuth are known, the orientation of the crystal relative to the electron beam is completly determined. It should be remembered that while electrons are reflected throughout an entire hemisphere, the reflected beam is comprised of those electrons which are reflected into the Faraday collector. Thus the plane of the incident and reflected electrons may also be thought of as the plane in which the Faraday collector is rotated.

In this investigation only the 0001 face was used. The analysis which follows will, therefore, deal with the azimuths of this face.

Figure 6 shows the arrangement of atoms in the $01\bar{1}0$ azimuth. The relative size of the circles indicates the arrangement of the atoms within the lattice. The positions of all the diffraction beams in this azimuth can be determined by considering three consecutive planes of atoms. Therefore, only these have been included in the figure.

The condition for constructive interference between electrons reflected from two atoms is that the path differance be equal to an integral number of wave lengths. Thus for the two atoms at the top left (figure 6) the path difference is

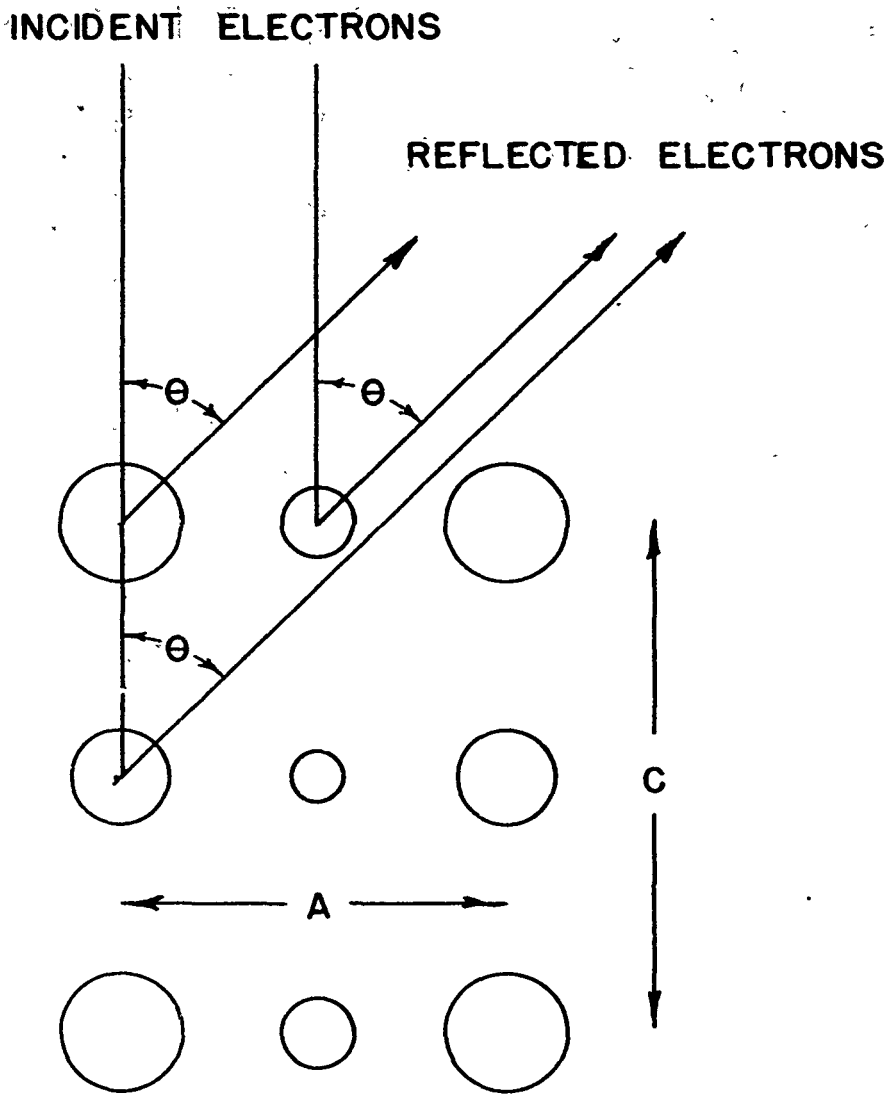

FIGURE 6

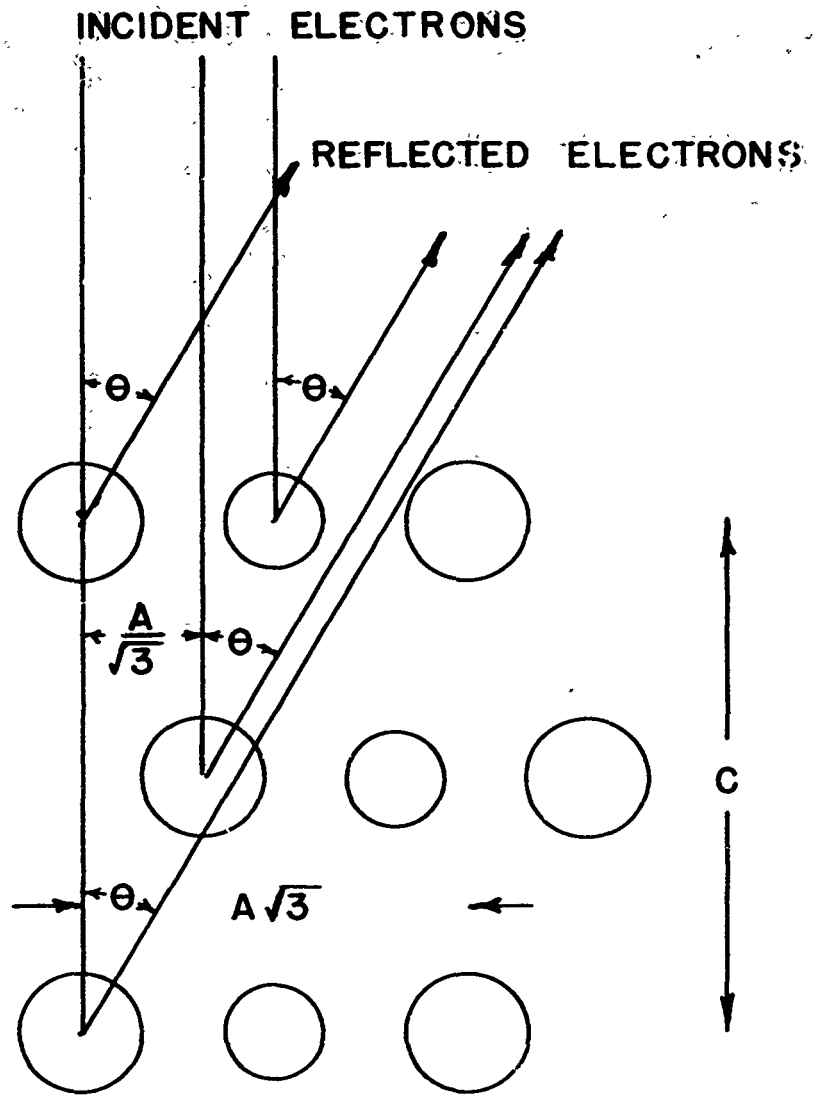

FIGURE 7

$$\delta = \frac{A}{2} \sin \theta.$$

Therefore

$$N_1 \lambda = \frac{A}{2} \sin \theta, \text{ for constructive interference.}$$

Substituting $\lambda = \sqrt{\frac{150}{V}}$ and $A = 2.950$ Å into the above equation, one obtains

$$V = \frac{68.9}{\sin^2 \theta} N_1^2, \tag{1}$$

for the relationship between V and θ at constructive interference.

For the atoms on the left side (figure 6) the path difference is

$$\delta = \frac{C}{2} (1 + \cos \theta),$$

Therefore

$$N_2 \lambda = \frac{C}{2} (1 + \cos \theta)$$

where $C = 4.683$ Å. Substitution of values for λ and C yields

$$V = \frac{27.3 N_2^2}{(1 + \cos \theta)^2}. \tag{2}$$

It should be noted that when the condition for constructive interference is satisfied between two atoms in the first layer, it is automatically satisfied for all atoms in the first layer. This situation is also present with respect to the constructive interference between atoms of the first and second layers. Extension of this idea leads to the conclusion that the diffraction conditions for the $01\bar{1}0$ azimuth of the 0001 face are completely determined by equations (1) and (2).

Figure 8 is a set of graphs of equations (1) and (2) for various values of V and θ. Each curve represents a particular value of N_1 or N_2. The intersections of these curves represent values of the parameters V and θ for which the constructive interference condition is satisfied between all atoms. It is reasonable to expect, therefore, that the intersections will correspond to maximum values of reflected electron current and hence, to the diffraction pattern itself.

Figure 7 shows the arrangement of the atoms in the $11\bar{2}0$ azimuth. Since the path difference is

$$\sigma = \frac{3}{2} A \sin \theta,$$

the condition for constructive interference between the two top atoms is

$$N_1 \lambda = \frac{3}{2} A \sin \theta,$$

or

$$V = \frac{5.72}{\sin^2 \theta} N_1^2 . \qquad (3)$$

Constructive interference between the top and bottom atoms in the same figure is satisfied when

$$N_2 \lambda = C(1 + \cos \theta),$$

or

$$V = \frac{N_2^2 150}{C^2 (1 + \cos \theta)^2} . \qquad (4)$$

The last set of atoms to be considered in this azimuth is that made up of the atoms in the top and center layers. In this case the interference condition may be expressed as

$$N_3 \lambda = \frac{C}{2} (1 + \cos \theta) = \frac{A}{\sqrt{3}} \sin \theta,$$

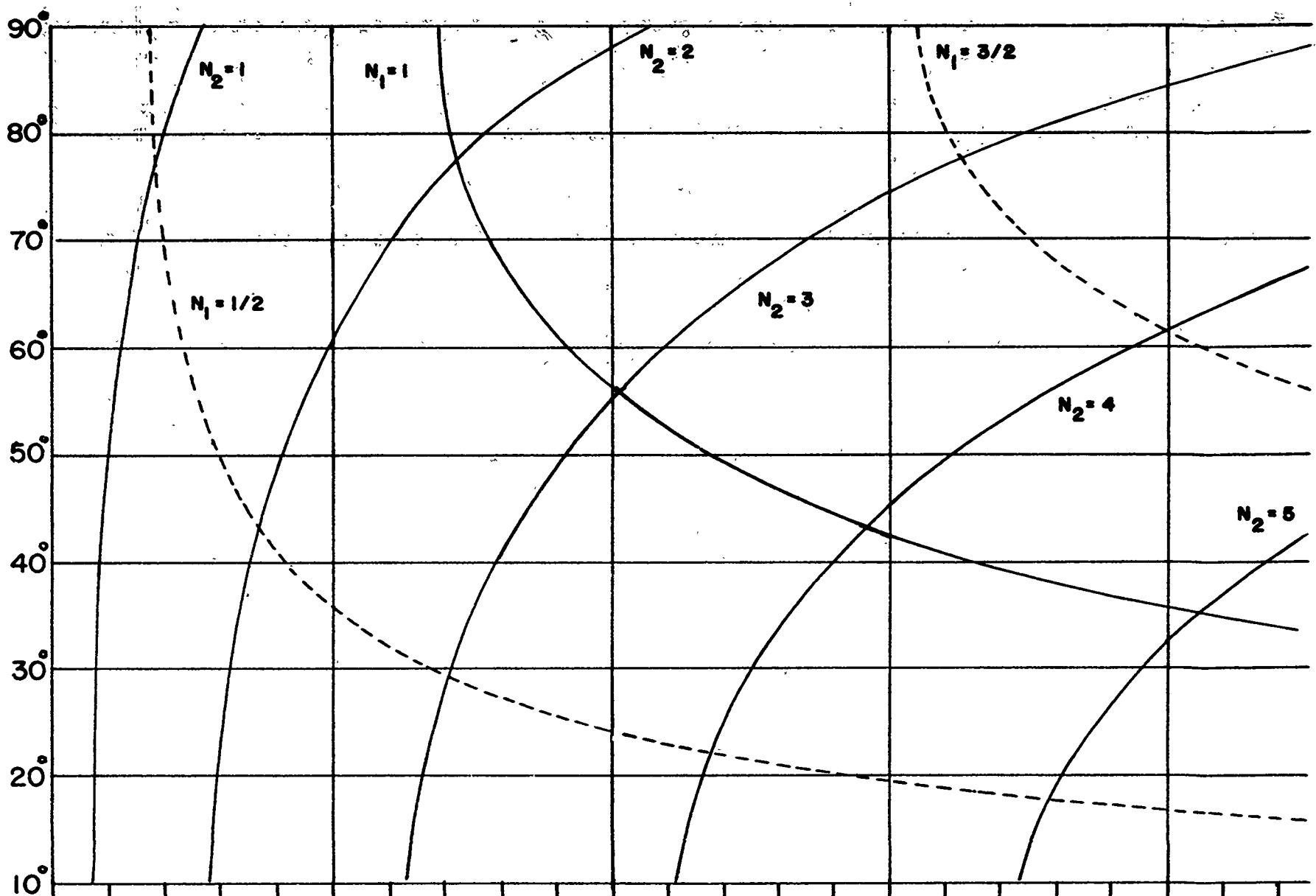
90°
80°
70°
60°
50°
40°
30°
20°
10°
0
50
100
150
200 VOLTS
N2=1
N1=1
N2=2
N1=3/2
N1=1/2
N2=3
N2=4
N2=5

FIGURE 8

or $$V = \frac{150\, N_3^2}{\frac{C^2}{4}(1+\cos\theta)^2 - \frac{CA}{\sqrt{3}}(\sin\theta)(1+\cos\theta) + \frac{A^2}{3}\sin^2\theta} \quad . \qquad (5)$$

Figure 9 is a set of graphs of equations (3), (4) and (5) for various values of V and θ. Each curve again represents a selected value of N_1, N_2 or N_3. The diffraction maxima are expected to occur at the intersections of these curves as in the case for the other azimuth.

Due to the asymmetry in the $11\bar{2}0$ azimuth (see figure 7), the diffraction pattern will not be symmetrical when negative values of θ are included. It is necessary, therefore, to calculate the conditions for constructive interference for negative values of θ. The only difference introduced by the assymetry lies in the interference condition between atoms in the top and center layers. This interference condition may be expressed as

$$N_4\lambda = \frac{C}{2}(1+\cos\theta) + \frac{A}{\sqrt{3}}\sin\theta,$$

or $$V = \frac{150\, N_4^2}{\frac{C^2}{4}(1+\cos\theta)^2 + \frac{CA}{\sqrt{3}}(\sin\theta)(1+\cos\theta) + \frac{A^2}{3}\sin^2\theta} \quad . \qquad (6)$$

Figure 10 is a set of graphs of equations (3), (4) and (6) for various values of V and θ. Each curve represents a selected value of N_1, N_2 or N_4.

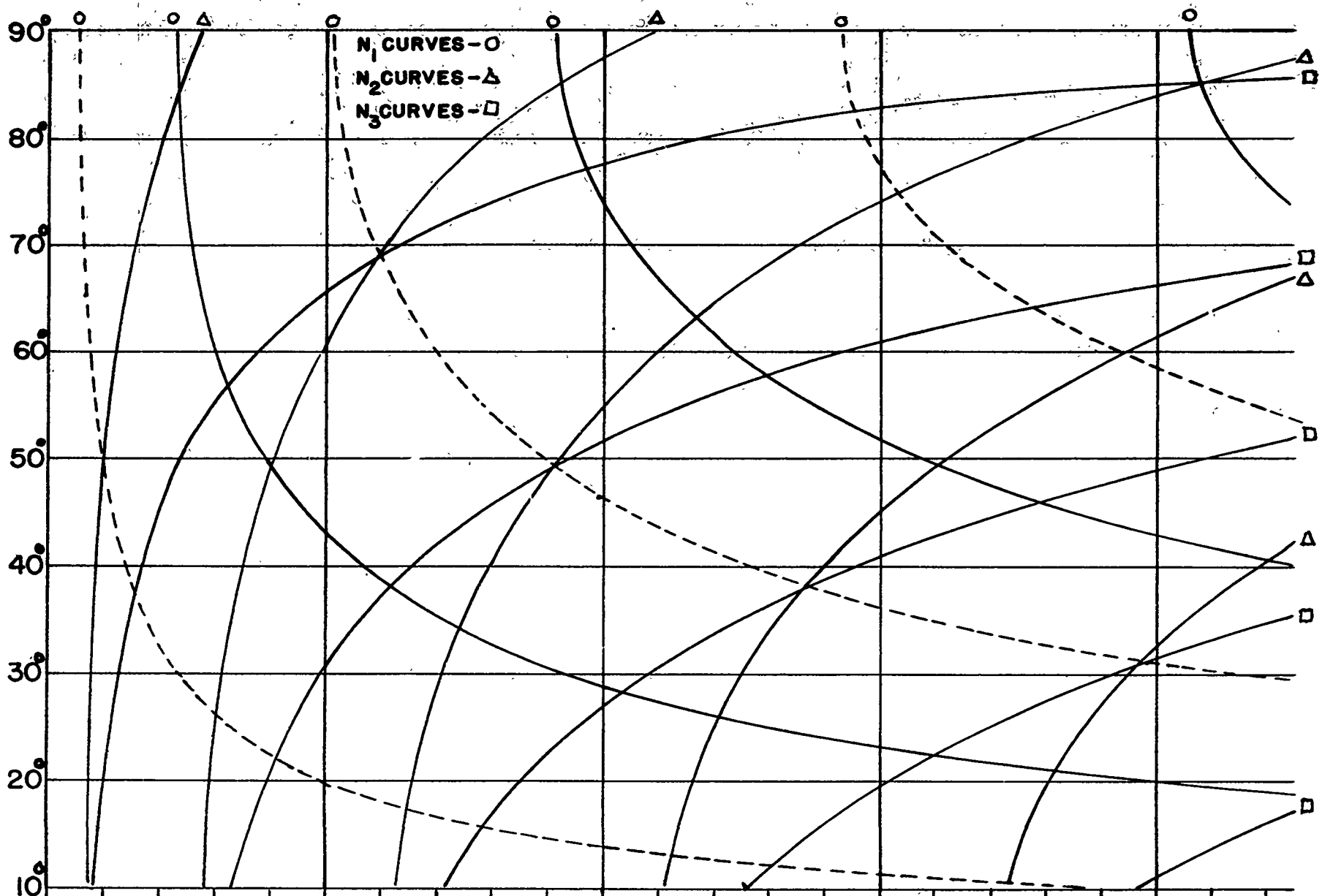
N1 CURVES – O
N2 CURVES – Δ
N3 CURVES – □
90°
80°
70°
60°
50°
40°
30°
20°
10°
0
50
100
150
200 VOLTS

FIGURE 9

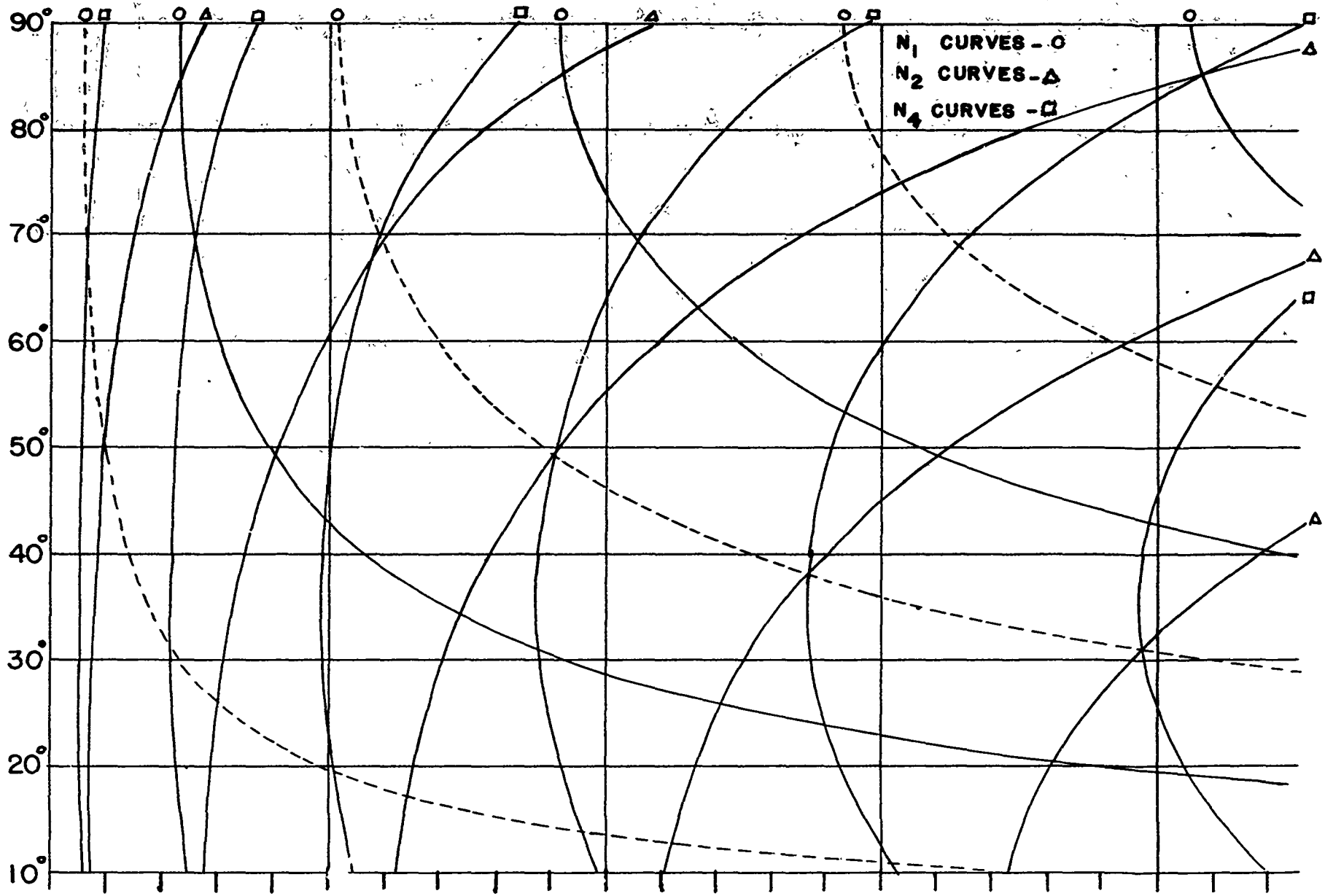
90°
80°
70°
60°
50°
40°
30°
20°
10°
0
50
100
150
200 VOLTS
N1 CURVES - O
N2 CURVES - Δ
N4 CURVES - □

FIGURE 10

THE VACUUM SYSTEM

The Requirements of the System It has been well established that titanium has a great affinity for most gases. This property has, in fact, been exploited to advantage in the use of titanium as a getter. This effect has been studied by many investigators. For example, Gulbransen and Andrew[8] reported that the reaction

$$Ti + H_2O + CO_2 \longrightarrow TiO_2 + H_2 + CO$$

takes place at temperatures up to 800°C. and higher at pressures of 10^{-7} mm. of mercury.

Information of this kind serves as an indication of the problems involved in outgassing a titanium crystal. Since higher temperatures cannot be attempted because of the alpha to beta transition mentioned earlier, any hope of reversing such a reaction lies in obtaining the lowest possible pressure.

An important consideration involved in the design of a vacuum system for electron diffraction surface studies is the possible contamination of the sample under investigation. Since little is known about the decomposition products of diffusion pump oils, it seemed desirable to use a pumping mechanism which introduced no contamination or, at worst, a known contaminant which could subsequently be controlled.

For this reason, an all-glass, mercury vapor diffusion pump vacuum system was designed. The mercury was purified in an oxifier and filtered before filling the pumps, and when liquid nitrogen was put in the traps there was no contamination introduced into the experimental tube since the vapor pressure of mercury at liquid nitrogen temperature (-190°C.) is 1.7×10^{-27} mm. of Hg.

In addition to the vacuum system proper it was necessary to design a gas inlet system so that purified gases could be released into the experimental tube over a wide range of pressures. It was also required that these pressures be maintained for relatively long periods of time. The way in which these last problems were solved is described in the next section.

The Completed System The final system is composed of Pyrex glass, each component having been cleaned at least once and in some cases four times by filling with a saturated solution of potassium dichromate in concentrated sulfuric acid for a period of not less than twelve hours. This was followed with five tap-water rinses and ten distilled water rinses after which the ends of each piece were covered with aluminum foil to keep out dust and the whole was dried in an oven at 150° C. All the components of the vacuum system were hung on a pipe framework separately and then sealed together, care being taken to anneal all the joints so that the whole assembly would be under as little strain as possible.

It should be noted that filter paper was substituted for aluminum foil for capping the ends of the glassware once mercury had been put into the system. It was found that the mercury vapor reacted with the aluminum foil to form a white powdery compound.

Figure 11A is a block diagram of the vacuum system. The inclusion of all four traps in one flask cuts down the liquid nitrogen loss and allows the vacuum system to operate unattended for three days. Both fore-volumes are five liters so that the pressure increase in the fore-volumes, once the system has been pumped down, is negligible over this period. The three mercury diffusion pumps are heated by external electric heaters. These heaters are normally operated on 110 volts a.c., but are connected by means of a relay to

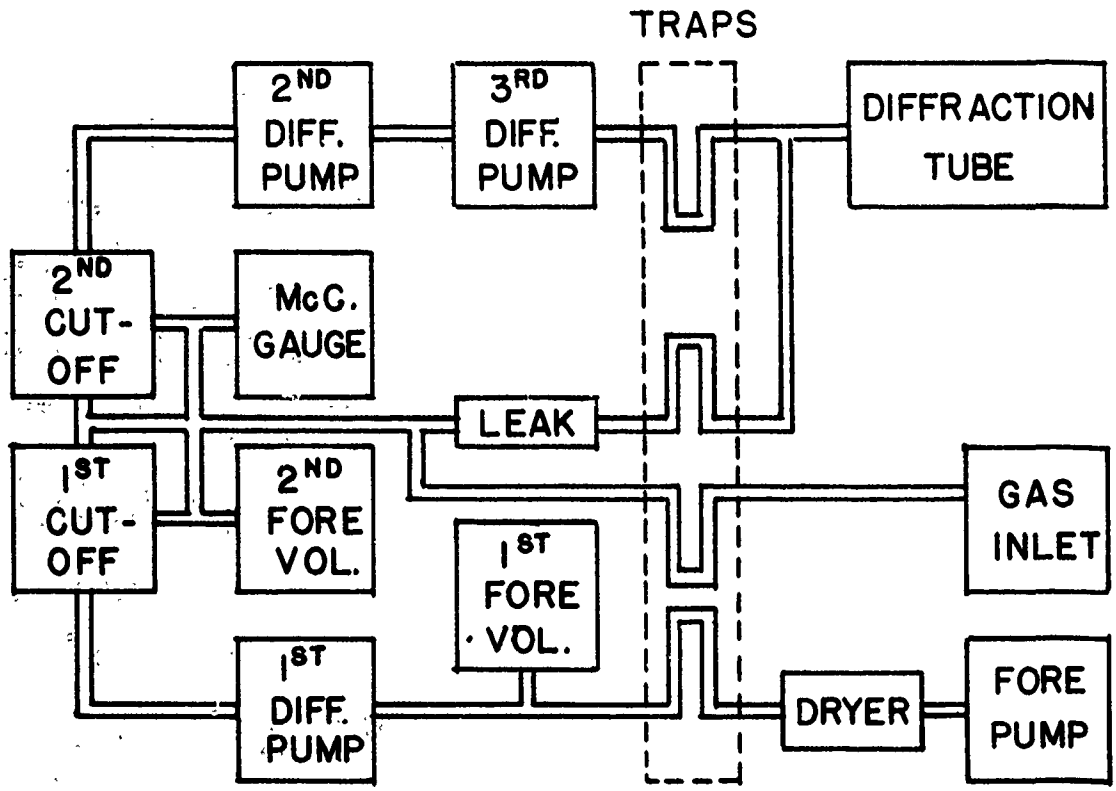

FIGURE IIA

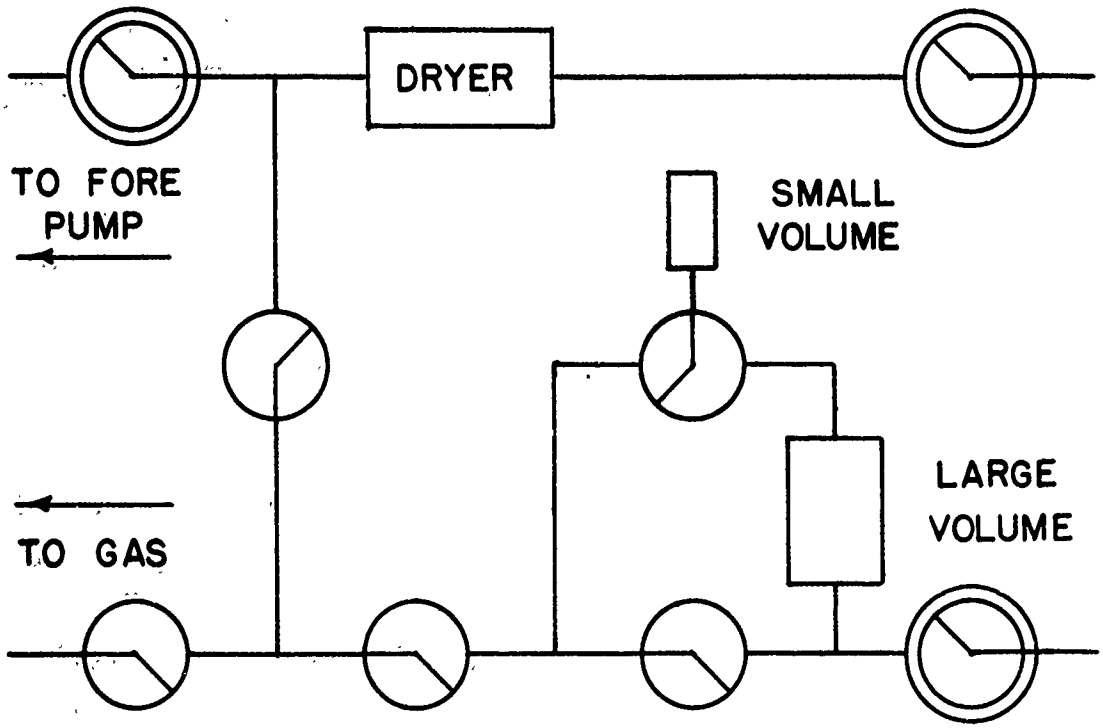

FIGURE IIB

stand-by batteries which will operate the pumps in the event of a power failure.

Figure 11B is a diagram of the arrangement of stopcocks which comprise part of the gas-inlet system. The top part of the figure represents the fore-pump line with double circles indicating vacuum stopcocks. The lower part of the figure represents the gas-inlet line. Two different size volumes allow different amounts of gas at atmospheric pressure to be released into the second fore-volume, making a wide range of fore-volume pressures more easily obtainable. The connection between the gas-inlet stopcocks and the fore-pump line allows the gas-inlet system to be evacuated with the fore-pump.

Figure 14 is a diagram of the mercury cutoffs. By raising and lowering the mercury reservoir, various pumping arrangements can be had. This configuration provides the following combinations.

	level of #1	level of #2	result
a)	(0)	(0)	evacuation of second fore-volume and experimental tube
b)	(1)	(1)	evacuation of experimental tube, second fore-volume isolated
c)	(0)	(2)	evacuation of second fore-volume, experimental tube isolated
d)	(2)	(0)	pumping from experimental tube to second fore-volume both isolated

These combinations have the following uses.

a) - initial evacuation of the system

b) - admission of gas into the second fore-volume

c) - evacuation of the second fore-volume

d) - circulation of gas for adsorption investigations

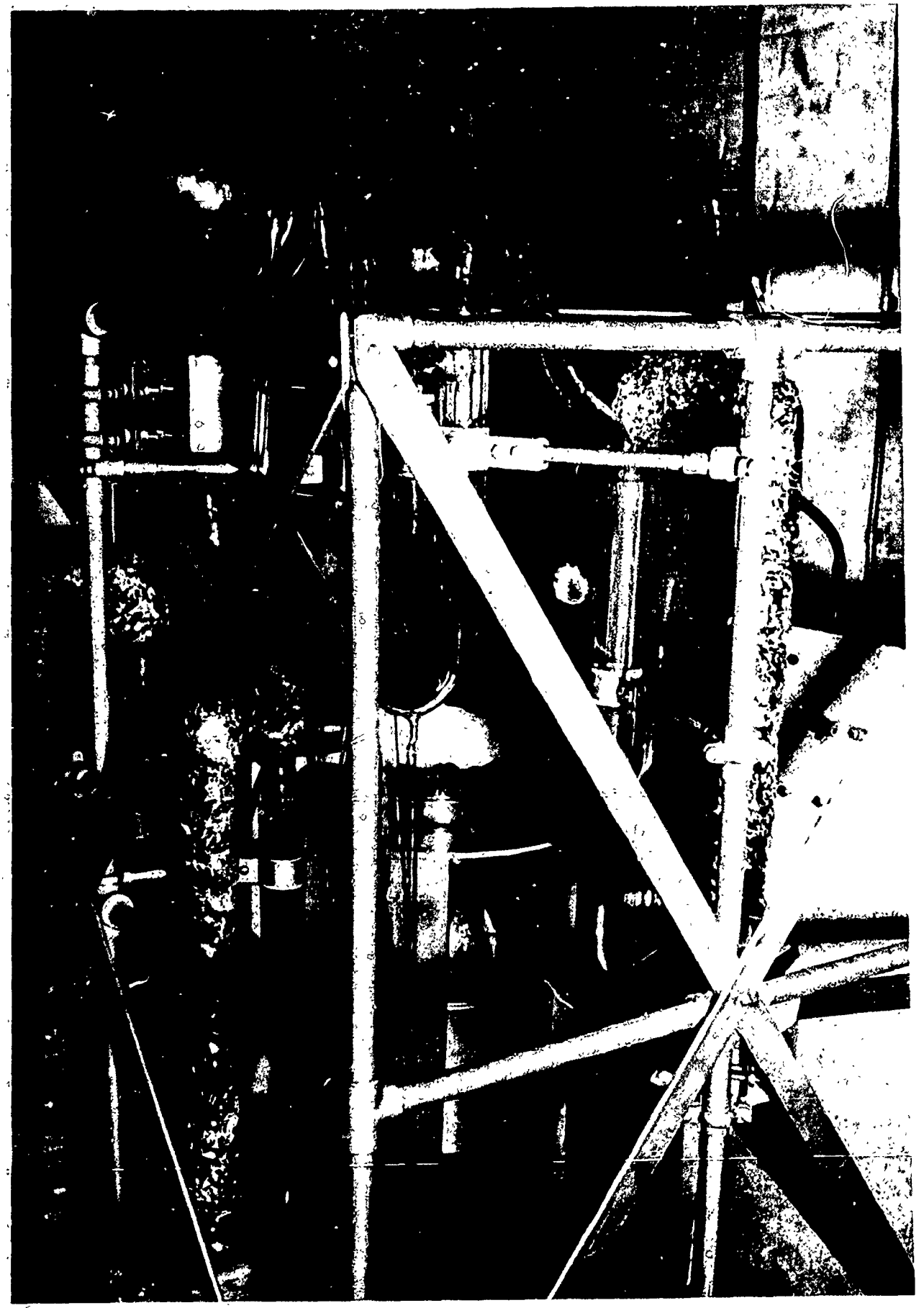

FIGURE 12

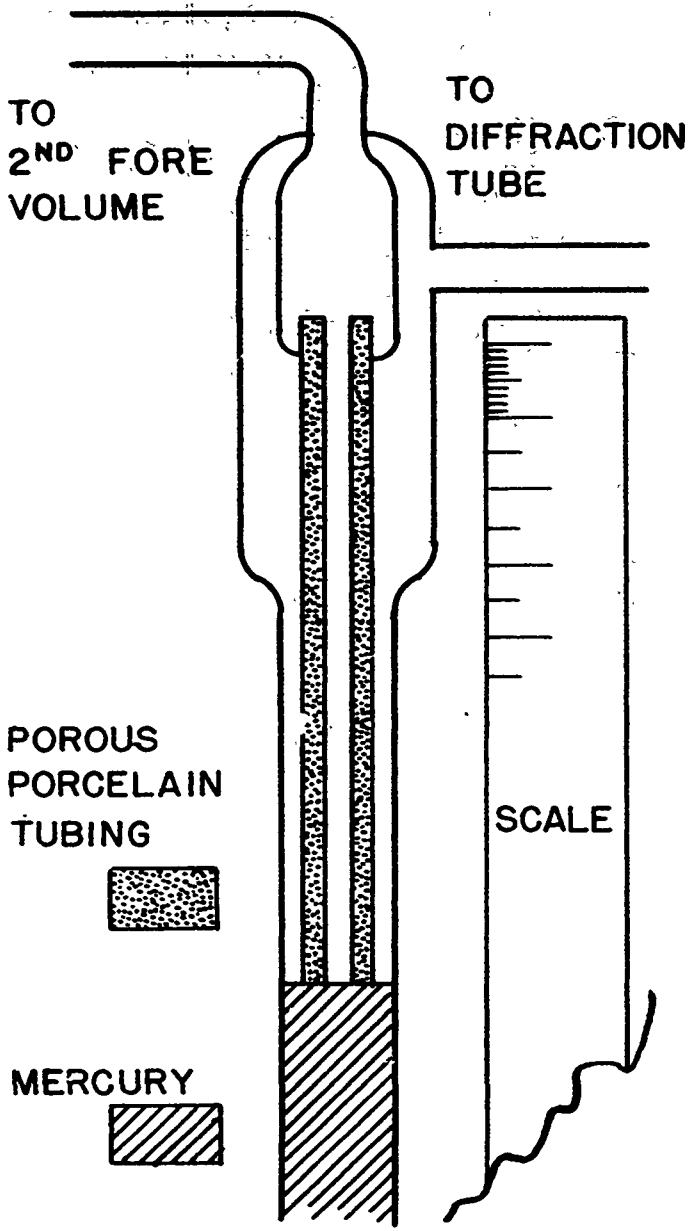

FIGURE 13

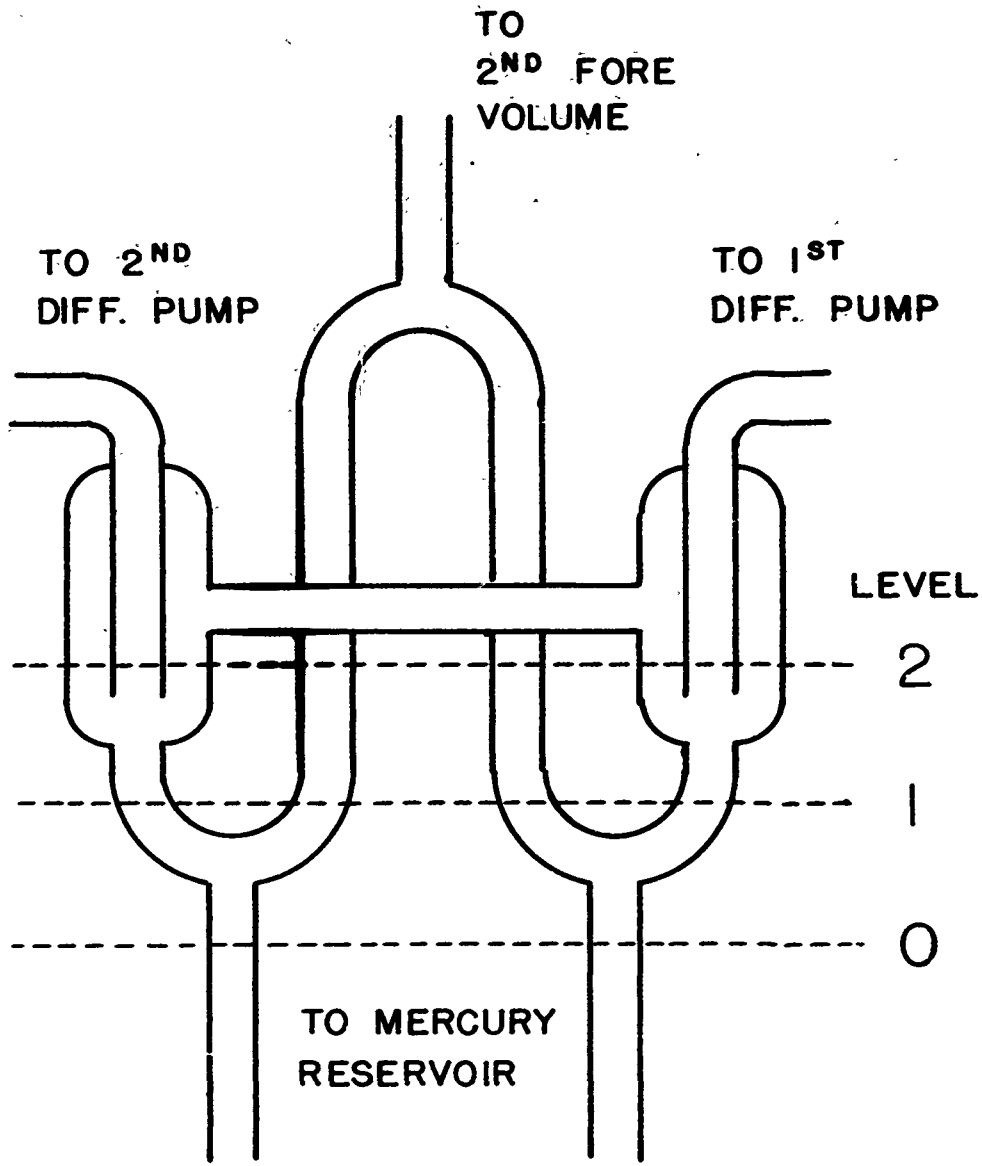

FIGURE 14

Figure 12 is a photograph of the vacuum system. The diffusion pumps (wrapped in aluminum foil to minimize heat loss) are from left to right numbers 3, 2 and 1.

Special Components Figure 13 is a diagram of the gas leak through which the test gases may be admitted to the experimental tube. It consists of an unglazed porcelain tube, sealed by a Nonex-Uranium-Pyrex graded seal to a lead from the second fore-volume. The porcelain tube extends below the level of the mercury in the surrounding glass tube. As the level of the mercury is lowered or raised, more or less of the porcelain is exposed varying the rate of gas flow from the second fore-volume, through the walls of the porcelain tube, to the experimental tube.

Figure 15 is a graph of the resulting tube pressure as a function of the length of porcelain tube exposed. Each of the curves represents a different fore-pressure.

By setting the cutoffs #1 - (2), #2 - (0), the gas is circulated back through pumps three and two into the second fore-volume and any pressure from 10^{-1} to 10^{-9} mm. of Hg. can be maintained in the experimental tube for any indefinite length of time. The accuracy with which the pressure can be adjusted is limited only by the accuracy of the gauge or gauges measuring it.

Four vacuum gauges have been incorporated into the vacuum system. One of these, a McCleod gauge, has a range from 10^{-1} to 10^{-6} mm. of Hg. and includes a closed tube manometer, reading from atmospheric pressure down to 1 mm. This gauge is connected directly to the second fore-volume and is used primarily for measuring the pressure of the test gas before adsorption runs are made. It may, however, be used to calibrate the Pirani gauge and the VG-1A ionization gauge

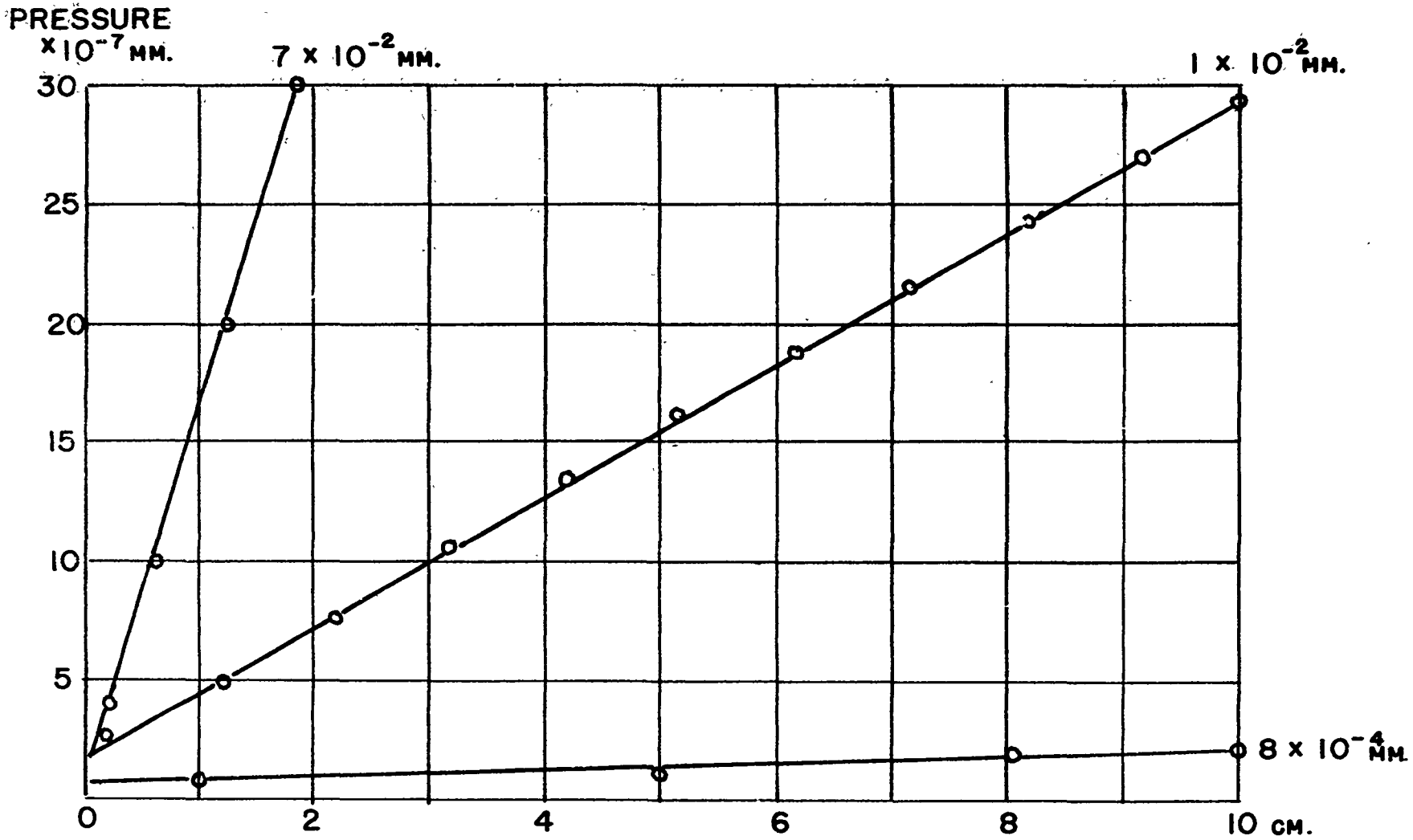

TUBE PRESSURE vs. LEAK OPENING

FIGURE 15

on the experimental tube. This is accomplished by opening the leak wide and waiting for equilibrium, under which condition the McCleod gauge will read the pressure in the experimental tube.

The Pirani gauge on the experimental tube is used to measure relatively high test-gas pressures and has a range from 10^{-2} to 10^{-4} mm. The second gauge on the experimental tube is a VG-1A ionization gauge used for measuring low tube pressures. This gauge has a range from 10^{-3} to 10^{-8} mm.

The third gauge, an ultra-high-vacuum (UHV) gauge on the experimental tube is an ionization gauge of new design, which, it is hoped, will measure pressures as low as 10^{-11} mm. This gauge is the M.I.T. version of the Bayard-Alpert type ionization gauge[9], which utilizes a thin wire as the ion collector.

Figure 16 is a photograph of the glass envelope of the experimental tube. The UHV gauge can be seen in the center of the picture suspended from the tube. The other gauges flank the bulb with the VG-1A on the near side and the Pirani gauge on the far side. The 30 inch diameter coils, visible in Figure 16, are Helmholtz Coils used to compensate the magnetic field of the earth.

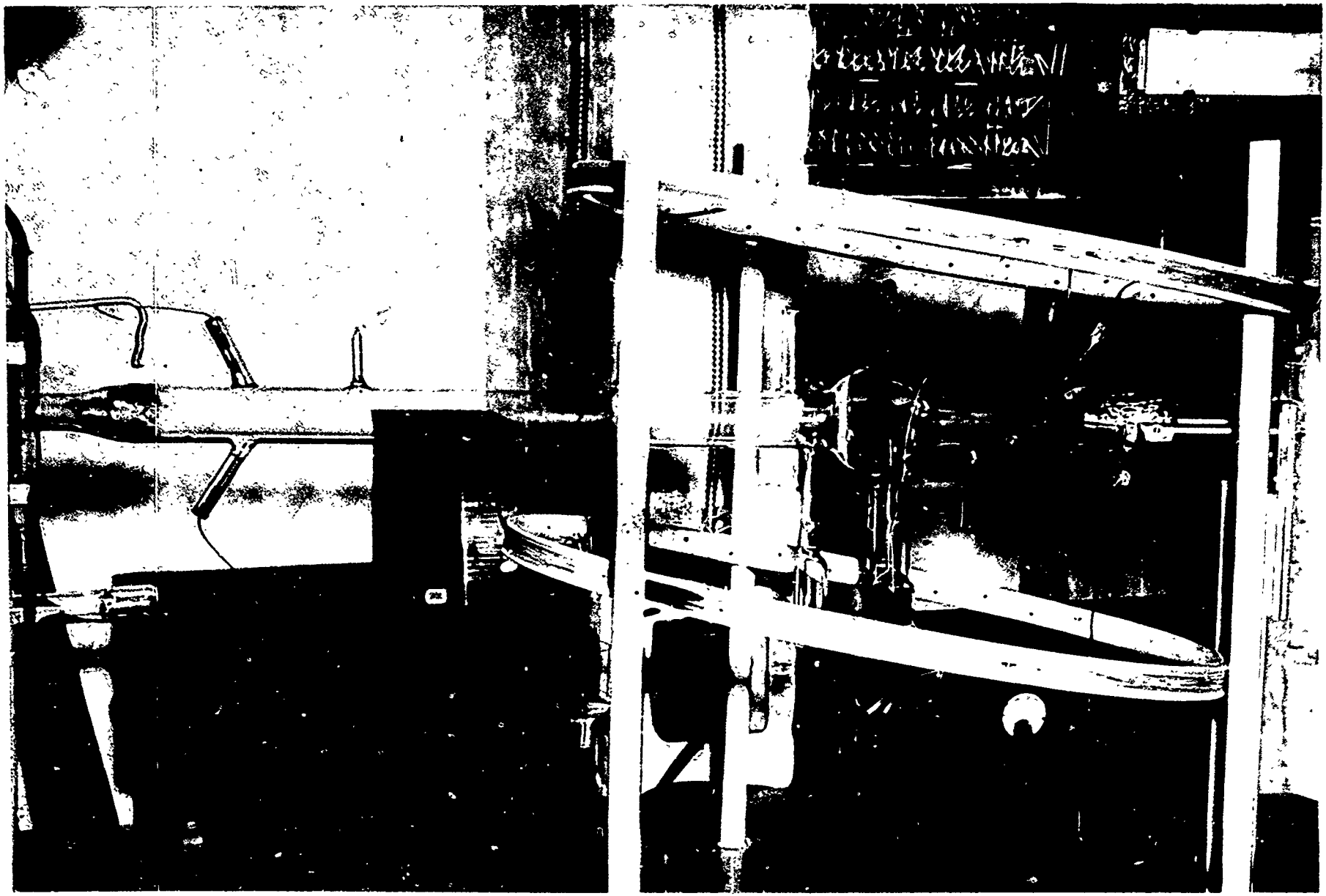

FIGURE 16

THE EXPERIMENTAL TUBE

Construction Techniques After the individual parts had been cut out according to specifications given on the parts drawings, they were fitted together in a trial assembly. This served two purposes: it indicated what alterations were necessary in order that the parts fit together easily and it allowed the assembler to become familiar with the operations involved. This was an important consideration as the final assembly had to be carried out without the parts being touched except with filter paper and specially cleaned tools.

Before the final assembly the parts were electro-polished in a solution consisting of 40% ortho-phosphoric acid and 60% glycerine. A strip of stainless steel served as the cathode. After the polishing was completed the parts were washed in hot tap water and then boiled in several rinses of distilled water.

The parts were then spot-welded together using clean molybdenum electrodes, taking care to handle them with clean tools only. Further precautions included the following. The scales, which could not be electro-polished without loss of clarity, were cleaned in ether of high purity. Quartz, which was used for its insulating properties, was heated to white heat just before the final assembly to minimize leakage. The glass rods and spacers were cleaned in the usual manner as described earlier.

The above procedures insured the absence of greases or other foreign matter from the experimental tube. These might have a high vapor pressure and thus make it impossible to obtain the best vacuum conditions, or might contaminate the crystal.

After the parts were assembled on the four glass rods, they were held together by bending a short right angle in one end of each rod and sealing an extra spacer

to the other end.

The Geometry Figure 17 is a photograph of the principle parts of the experimental tube. All metal parts unless otherwise noted were constructed of Chromel A. The metal parts were strung on four Pyrex rods (4 mm.) and were separated by means of spacers cut from Pyrex tubing (7 mm.).

The drum, which provides an electrostatic shield for the crystal, can be seen just to the left of center in the photograph. The Faraday collector box which collects the reflected electrons rotates around the drum and can be set at any angle from 15 to 90 degrees with respect to the axis of the experimental tube. The scale, provided for reading the collector box (colatitude) angle, may be seen on the opposite side of the drum.

To the right of center is the electron gun. This gun was designed[10] to provide a well collimated monochromatic beam of electrons. The electron emitter (tungsten strip) is located off the axis of the tube so that contamination which might be introduced by evaporation from this emitter would not reach the crystal.

The smaller glass tubes apparent on the right side of the photograph provide an insulated path for the various potential leads.

The cutaway drawing shown in figure 18 gives an insight into the operation. Electrons leave the collimator shown on the right, enter the drum through the slot in the front and are reflected into the Faraday collector, as indicated by the arrows.

The collector is composed of two approximately rectangular boxes insulated from each other by thin quartz plates. The electrons enter through coaxial holes cut through the outer and inner boxes. These holes are 1 mm. and 2 mm. in diameter, respectively. The lead to the inner box (wavy line at the top of the

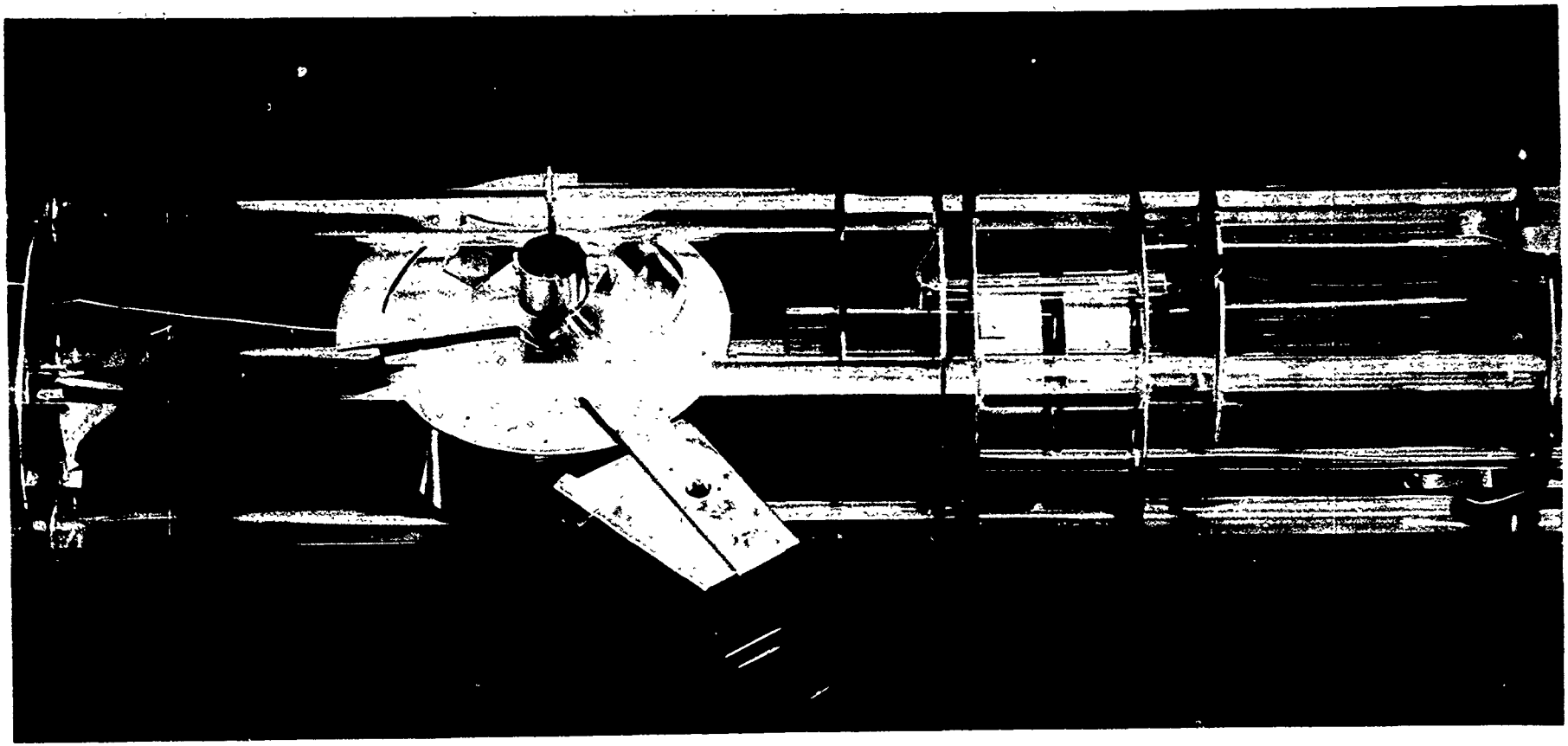

FIGURE 17

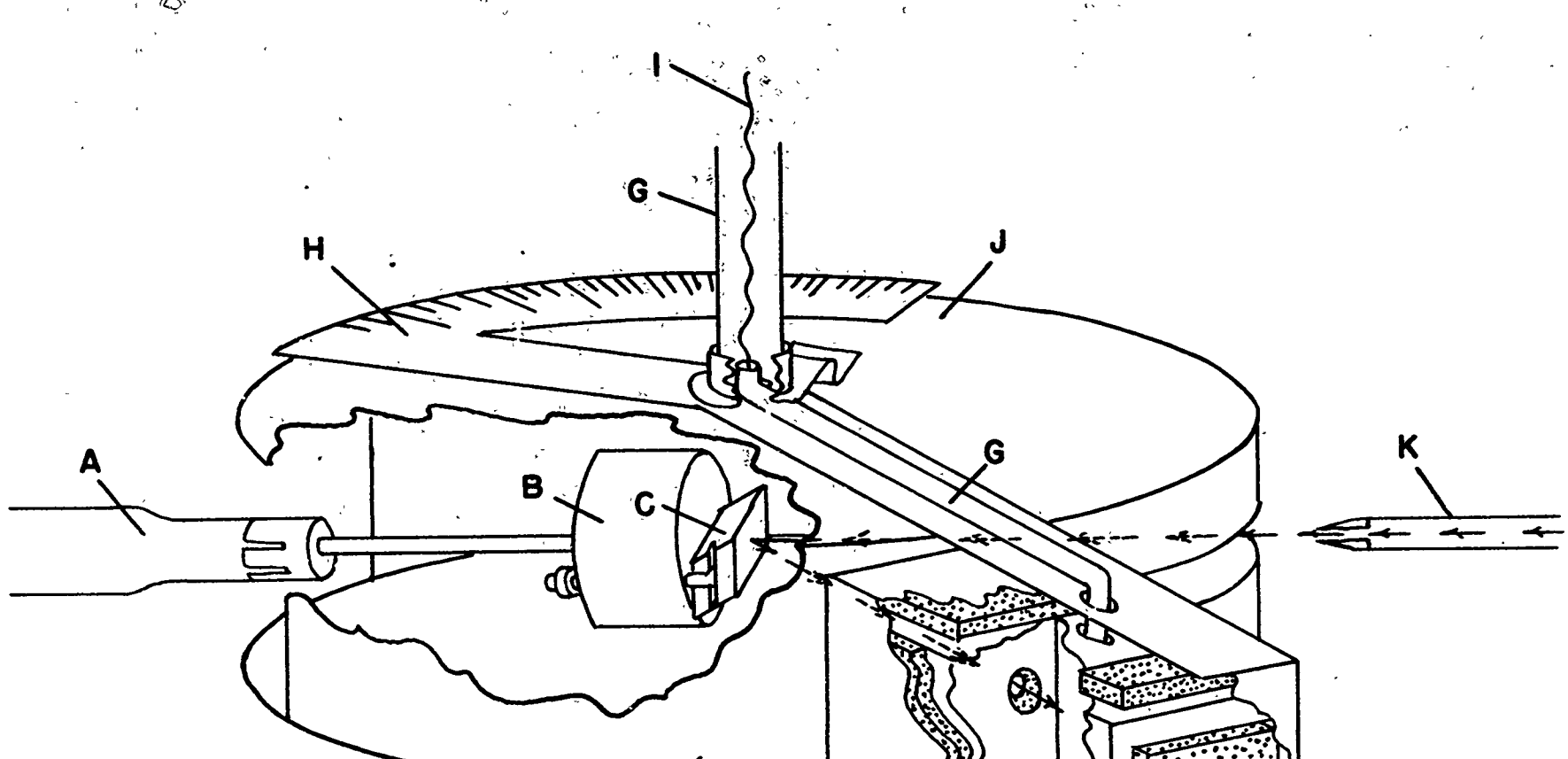

A - GLASS TUBE
B - MOLYBDENUM MOUNT
C - CRYSTAL
D - OUTER BOX
E - INNER BOX
F - QUARTZ INSULATION
G - QUARTZ TUBE
H - SCALE
I - LEAD TO INNER BOX
J - DRUM
K - COLLIMATOR
⟶ - ELECTRON PATH

FIGURE 18

drawing) is surrounded by quartz tubes from its origin at the re-entrance seal (not shown) to its terminus in the inner box. This provides insulation from the other metal parts as well as shielding from stray electrons. The whole collector assembly can be rotated by means of a chromel rod connected to a nickel slug (not shown) which is sufficiently far from the drum assembly to obviate any magnetic effects in the region of the electron beam.

The crystal shaft and mount are also operated by means of a magnetic control. This consists of another nickel slug located at the far end of the shaft (glass tube). Here again the shaft is long so that the nickel will have a negligible effect upon the magnetic field in the vicinity of the crystal. This control permits the crystal to be rotated for different azimuth settings (for which another scale is provided) and also allows the crystal to be withdrawn from the drum for bombarding.

The Electrical Circuit

Figure 19 is a schematic diagram of the electrical circuit. The multi-gang switch in the center of the drawing has three positions which correspond to the three principal configurations: shut-down, electron diffraction and contact potential.

The position shown in the drawing corresponds to shut-down. In this case all the tube parts are maintained at the reference potential which is -3 volts.

The next switch position is used for the diffraction measurements. In this case the crystal and drum are connected to the galvanometer so that the electron current to them can be measured. The collimator is set for the desired accelerating potential as read on the voltmeter. The two anodes of the electron gun are maintained at $67\frac{1}{2}$ volts positive with respect to the filament and the deflector is set in the neighborhood of 100 volts negative.

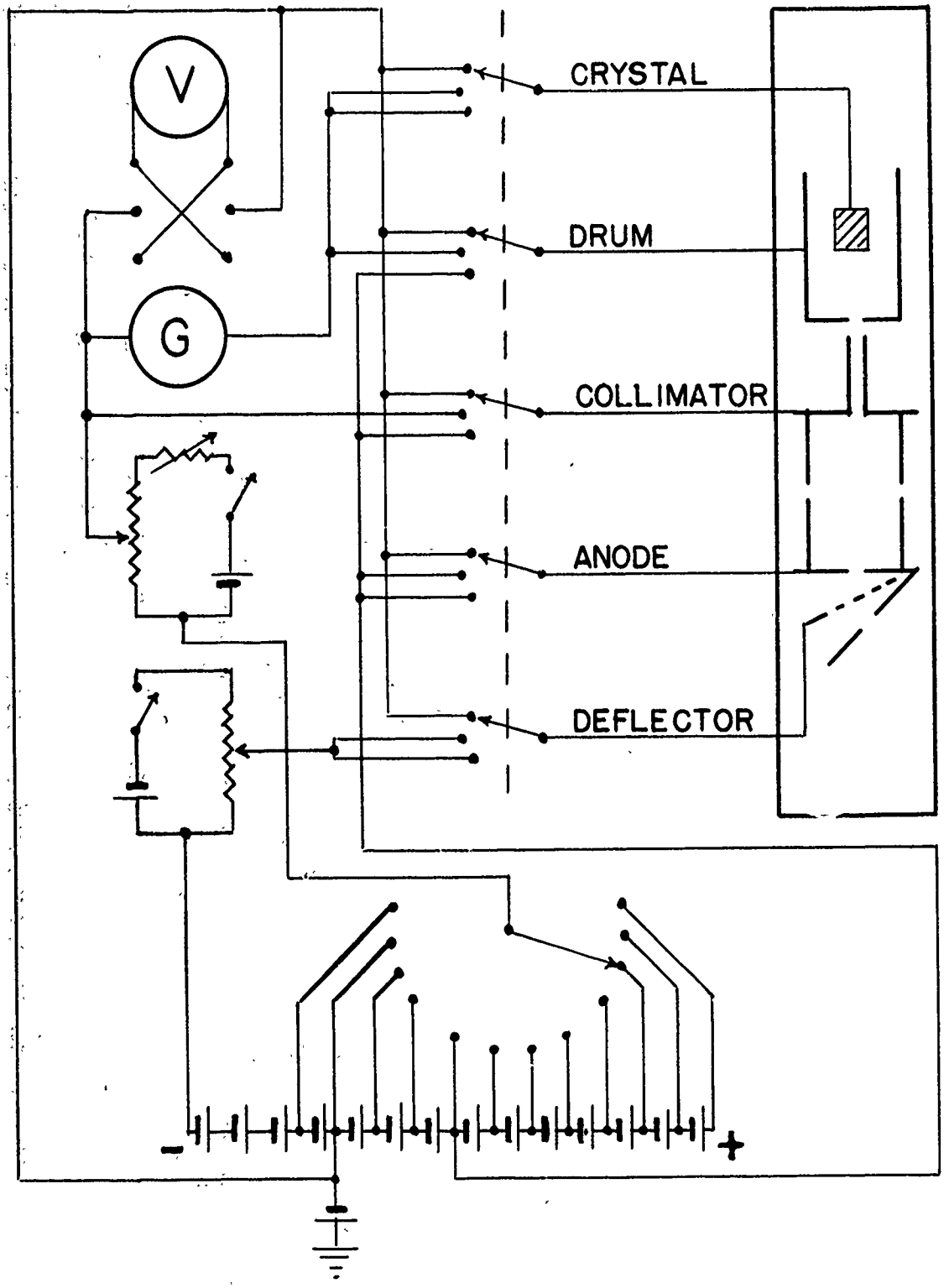

FIGURE 19

The collector box is operated at a retarding potential so that only those electrons enter the inner box which were elastically scattered from the crystal. The current to the inner box is measured by means of a d.c. amplifier of sensitivity 10^{-14} amps per millimeter galvanometer deflection.

The third position ties the drum, collimator, anode and deflector to $67\frac{1}{2}$ volts positive and allows the crystal potential to be varied. This arrangement is used for contact potential measurements by the electron gun method[11]. This method consists in observing the current to the crystal as a function of crystal potential, with all other variables fixed. An increase in work function (expressed in electron volts) of the crystal requires the crystal potential to be increased by the corresponding voltage, in order to obtain the original crystal current.

PRELIMINARY RESULTS

Since the experimental tube has been in operation for only a relatively short time at this writing, the results discussed here cannot be considered conclusive. A much more thorough investigation is required before definite statements concerning the surface structure can be made.

Method of Operation

At any one stage in the outgassing of the crystal there are four principal variables involved in the determination of the diffraction pattern, provided that the electron current to the crystal and drum is held constant throughout the investigation. These variables are the azimuth angle, the colatitude angle, the electron beam voltage (or wavelength) and the reflected electron current (usually referred to as the deflection). During an investigation the procedure consists in holding two of the first three variables constant and measuring the change in the deflection as a function of the third.

At each value of voltage the current to the drum and crystal was maximized with respect to the potential on the deflecting electrode of the electron gun. Throughout the investigations the Helmoholtz coils were operated at the current required to compensate for the earth's magnetic field as indicated by previous tests with a dip needle.

Before the experimental tube was operated it was baked for several hours at a temperature of 350°C. using electrical heating tapes which were wrapped around the envelope. The tube pressure after baking was approximately 3×10^{-7} mm. of mercury while the envelope was still hot.

Changes in the Diffraction Beams with Outgassing

In order to observe the change of a diffraction beam with outgassing, the location of a

principal beam was estimated. This was accomplished by approximating the setting of the azimuth angle corresponding to the $01\bar{1}0$ azimuth, on the basis of the final X-ray photograph (figure 3D). Reference was then made to the theoretical curves for this azimuth (figure 7) in order to obtain the voltage which corresponds to a theoretical beam. It was decided that 135 volts offered one of the best possibilities.

Figure 20A is a curve representing the variation in reflected electron intensity as a function of colatitude angle. This curve was taken before any outgassing of the crystal was attempted, and it shows the usual cosine dependence of the reflected intensity upon colatitude angle.

Figure 20B is a curve taken at the same voltage and azimuth angle, but after the crystal had been bombarded for 50 hours at 3 watts (450°C.). Irregularities in the region of 40 degrees indicate that a large part of the gas agglomerated on the surface of the crystal has been removed allowing the more regularly oriented atoms to alter the deflection. The tube pressure prior to the end of this bombarding was approximately 2×10^{-7} mm. of mercury.

Figure 20C is a third curve taken at 135 volts and at the same azimuth setting. This shows the effect of bombarding for 6 hours at 9 watts (700°C.). The 40 degree beam has been strengthened considerably and another beam has appeared in the neighborhood of 20 degrees. The tube pressure at the end of this outgassing period, with the crystal at 700°C , was approximately 2×10^{-7} mm. of mercury.

Additional outgassing for 24 hours at 720°C. had little effect upon this beam although it strengthened other beams which will be discussed below The tube pressure at the end of this outgassing period (the last prior to this

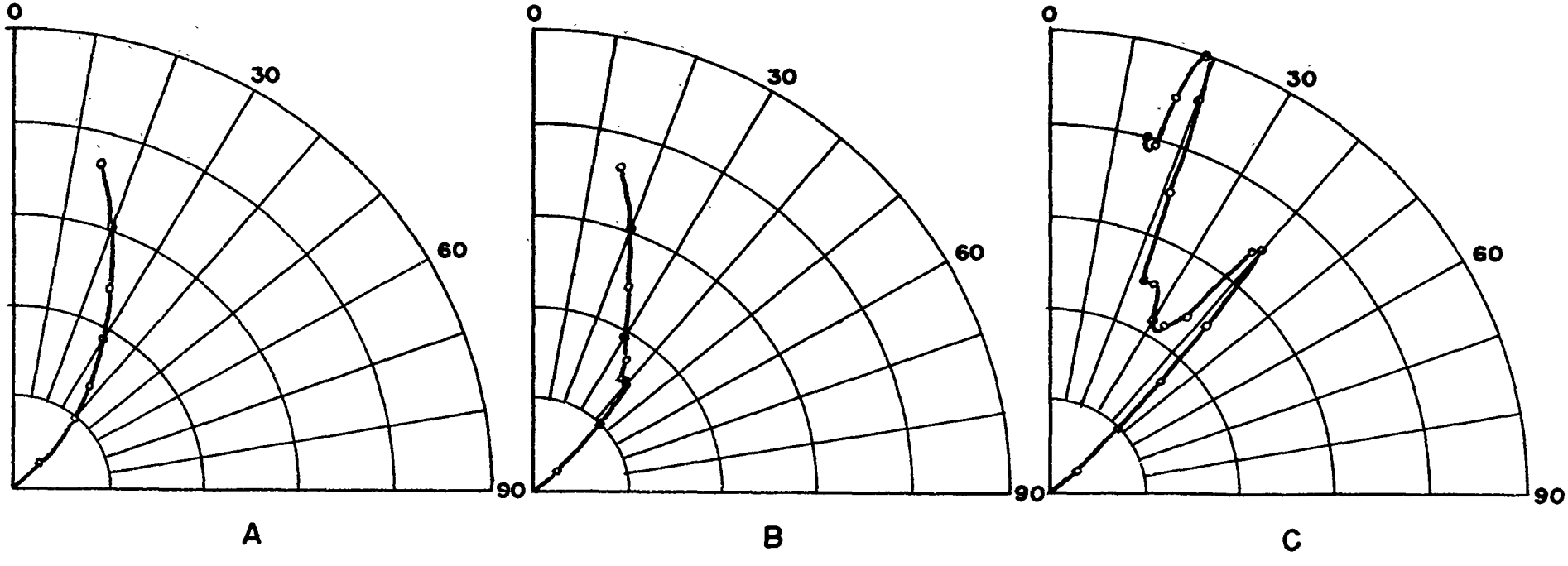

OITO AZIMUTH
135 VOLTS

FIGURE 20

writing) was 9×10^{-8} mm. of mercury with the crystal at 720°C.

Peak Variation with Voltage — After the above outgassing a random search for diffraction peaks indicated that several lay along the dotted curve $N_1 = \frac{1}{2}$ (figure 7). Further investigation showed another set which fitted the $N_1 = 1$ curve in the same figure. On the basis of this it was tentatively assumed that the diffraction beams corresponded to the $01\bar{1}0$ azimuth. Further investigations have thrown some doubt upon this conclusion as will be shown later.

It was decided, however, that a thorough investigation of the variation in peak intensity with voltage should be made. The $N_1 = \frac{1}{2}$ curve was the subject of this investigation with the result shown in figure 21A. At each value of voltage the colatitude angle was varied until a maximum deflection was obtained. The crosses indicate the colatitude angle at which these maxima occurred and the circles show the relative intensity of the reflected electron current (deflection). The four maximized peaks occur at

35 volts - 40 degrees

67½ volts - 28 degrees

82½ volts - 25 degrees

105 volts - 23 degrees.

Another principal peak not shown in the figure was found at

95½ volts - 60½ degrees.

The fact that the positions of the maxima followed the N_1 surface curve for the half order indicates that the diffraction pattern was the result of an arrangement of atoms in the surface plane and that these maxima resulted from some structure other than that of titanium, such as a double spaced gas layer.

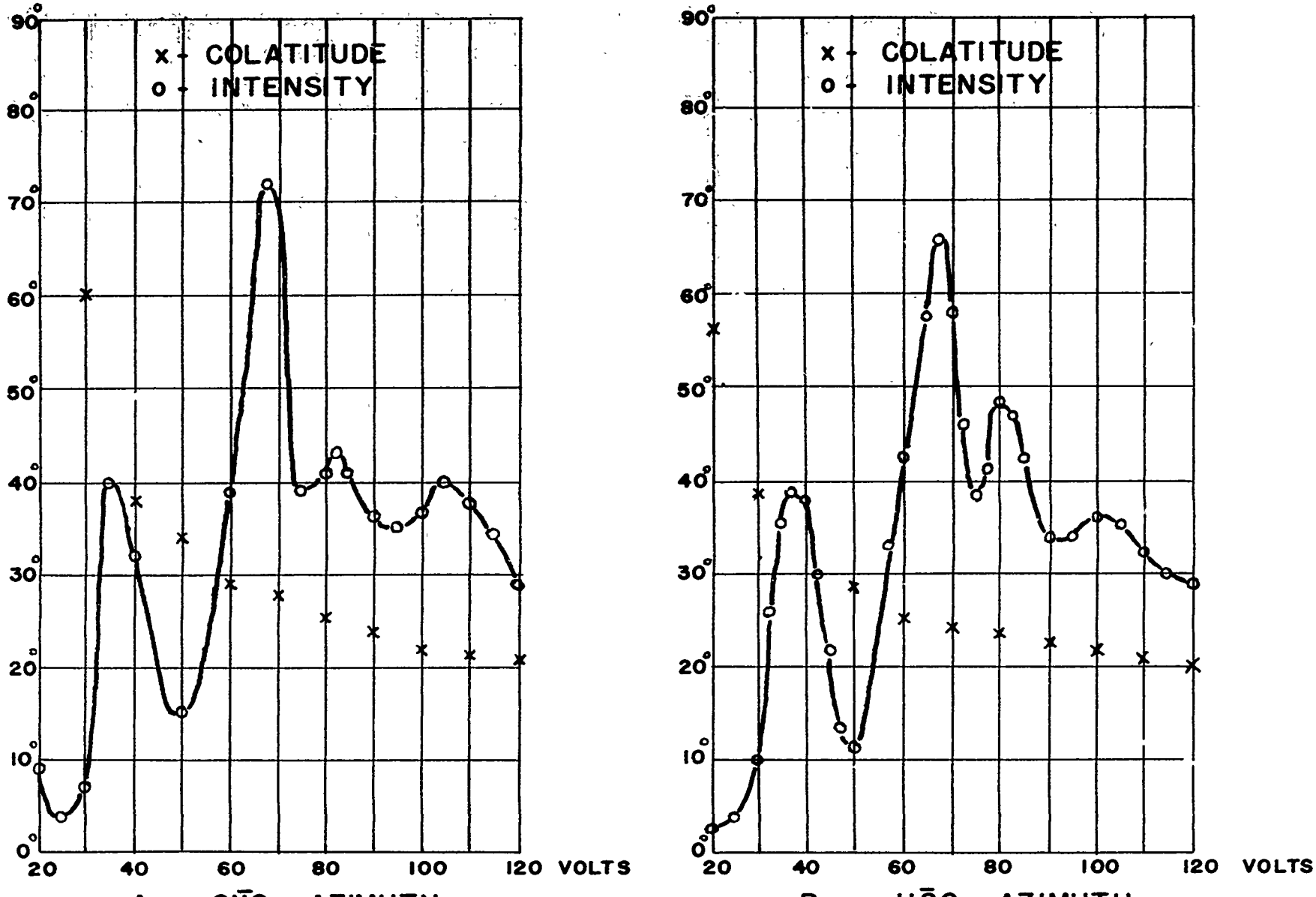
x - COLATITUDE
o - INTENSITY
90°
80°
70°
60°
50°
40°
30°
20°
10°
0°
20
40
60
80
100
120 VOLTS
A 01$\bar{1}$0 AZIMUTH
x - COLATITUDE
o - INTENSITY
B 11$\bar{2}$0 AZIMUTH

FIGURE 21

On the basis of this tentative hypothesis the azimuth angle was changed by rotating the crystal 90 degrees. It was expected that this would correspond to the $11\bar{2}0$ azimuth for which the theoretical curves are given in figures 9 and 10.

After a peak had been found in the same region as those in the other azimuth, the same voltage maximizing procedure was repeated with the results shown in figure 21B. In this azimuth the four maximized peaks occur at

$37\frac{1}{2}$ volts - 34 degrees

$67\frac{1}{2}$ volts $-27\frac{1}{2}$ degrees

80 volts -25 degrees

$102\frac{1}{2}$ volts -23 degrees.

At this point the remarkable similarity between the two curves (figure 21A and B) was noticed. Not only did the peaks follow the same surface curve and occur at the same voltages, but the intensity curve in B was a good repetition of the intensity curve in A. To substantiate the similarity a search was made for the fifth peak found in the other azimuth with the result that a peak was found in the $11\bar{2}0$ azimuth at

$92\frac{1}{2}$ volts - $59\frac{1}{2}$ degrees.

Spot checks of peaks at an azimuth angle setting 30 degrees from the original setting contributed additional evidence to the fact that the entire diffraction pattern was repeating every 30 degrees in azimuth rather than every 60 degrees as the hexagonal structure predicts.

The Azimuthal Curve. At this stage in the investigation it was decided that one of the most definite ways to settle the question of the repetition of the pattern every 30 degrees would be to select one diffraction maximum and study its behavior as the azimuth angle was changed in

small steps. This was accomplished in the following manner. The voltage was set at 67½ volts and held constant, and the crystal was rotated a few degrees at a time. At each setting the deflection was maximized with regard to colatitude angle. Figure 22A is a colatitude plot of the peak investigated and figure 22B is a plot of the peak intensity for various values of azimuth angle. The twelve-fold symmetry in the pattern is immediately apparent.

Since this curve took several days to complete, corrections were made for intensity changes over this period. This was accomplished by referring to former values of intensity which had been established in earlier portions of the curve. These corrections have been incorporated into the plot.

The Question of Twelve-fold Symmetry

When considering the foregoing data, one should not conclude that the arrangement of atoms on the surface of the crystal exhibits twelve-fold symmetry. In the first place such a conclusion would lead to the necessity of assigning a unique axis of rotational symmetry to the array. This situation is highly unlikely as it violates one of the principles of crystal structure, namely the requirement that any atom may be used as the origin of the coordinate system which describes the array. In addition such a postulate would require that the axis of rotational symmetry coincide with the axis of the shaft on which the crystal is mounted, and, furthermore, that the electron beam lie along this same axis regardless of the azimuthal angle through which the crystal is rotated. Since it is highly unlikely that any one of these requirements is satisfied in the experimental apparatus, the possibility of twelve-fold symmetry may be eliminated at once.

This does not mean, however, that the diffraction pattern cannot exhibit twelve-fold symmetry, as the requirement for this must be stated in a different way. This stems from the fact that the diffraction pattern for a given azimuth

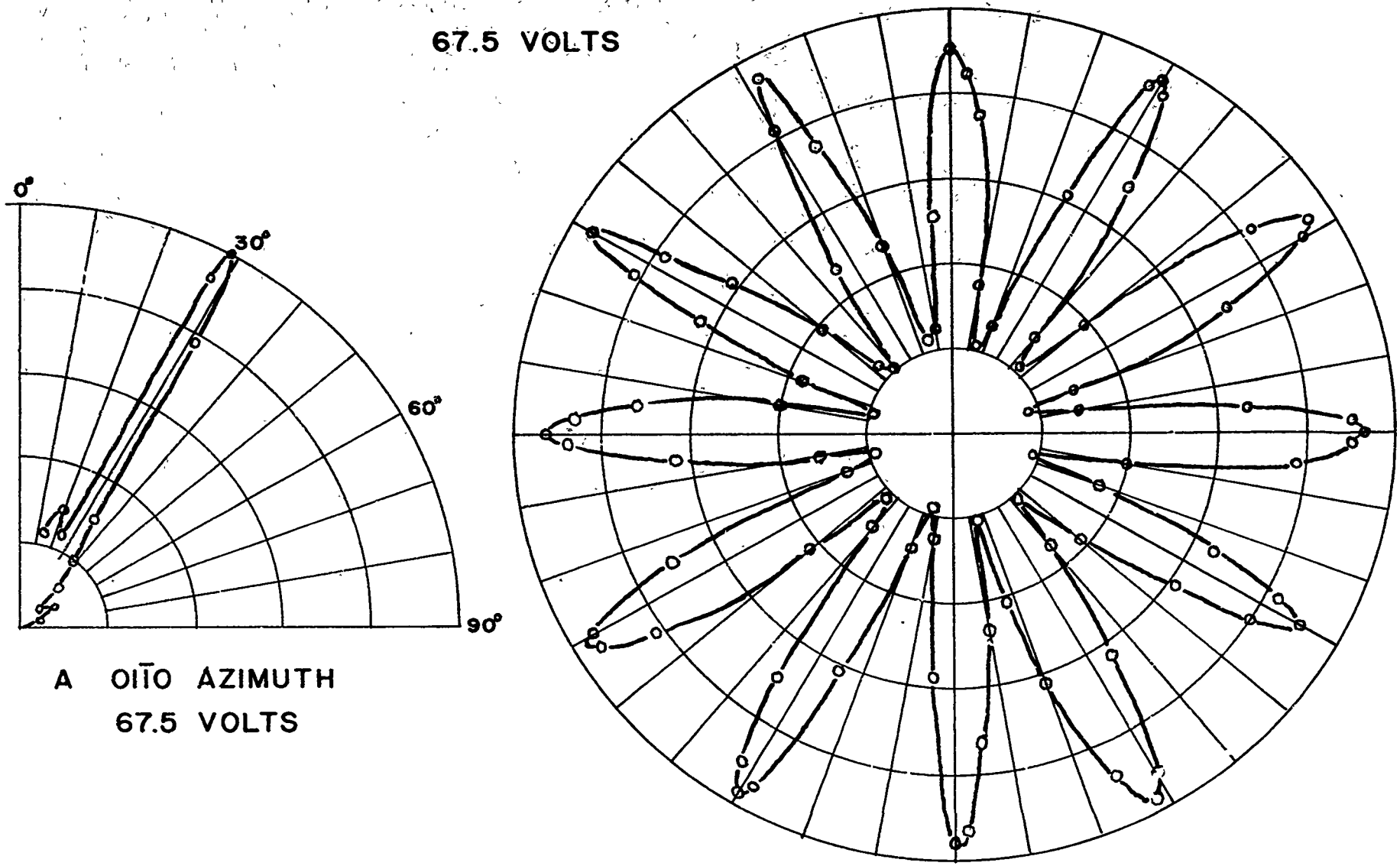

A OIIO AZIMUTH
67.5 VOLTS

B 28° COLATITUDE
67.5 VOLTS

FIGURE 22

is determined by the projection of the atoms onto the azimuthal plane. The question, essentially, is the following one. Does there exist an arrangement of atoms in a plane such that the projections of these atoms onto a set of lines, which are 30 degrees apart and lie in the same plane, produce a set of equally spaced points whose separation is the same along each line? It has been demonstrated mathematically that no such arrangement exists*. Much further investigation is required before the arrangement of the surface atoms can be determined.

Prospective While a multitude of investigations on the titanium crystal lie ahead, there are two more imminent than the rest. First, the completion of the study of the diffraction pattern that exists at this time, and second, an attempt to outgas the crystal further, not by heating to a higher temperature, as the alpha to beta transition prohibits this, but by obtaining lower pressures in the experimental tube.

It is to be hoped that the present results will appear more conclusive in the light of those which are to follow.

* William Lister, Assistant Professor of Mathematics, Brown University. (Private Communication)

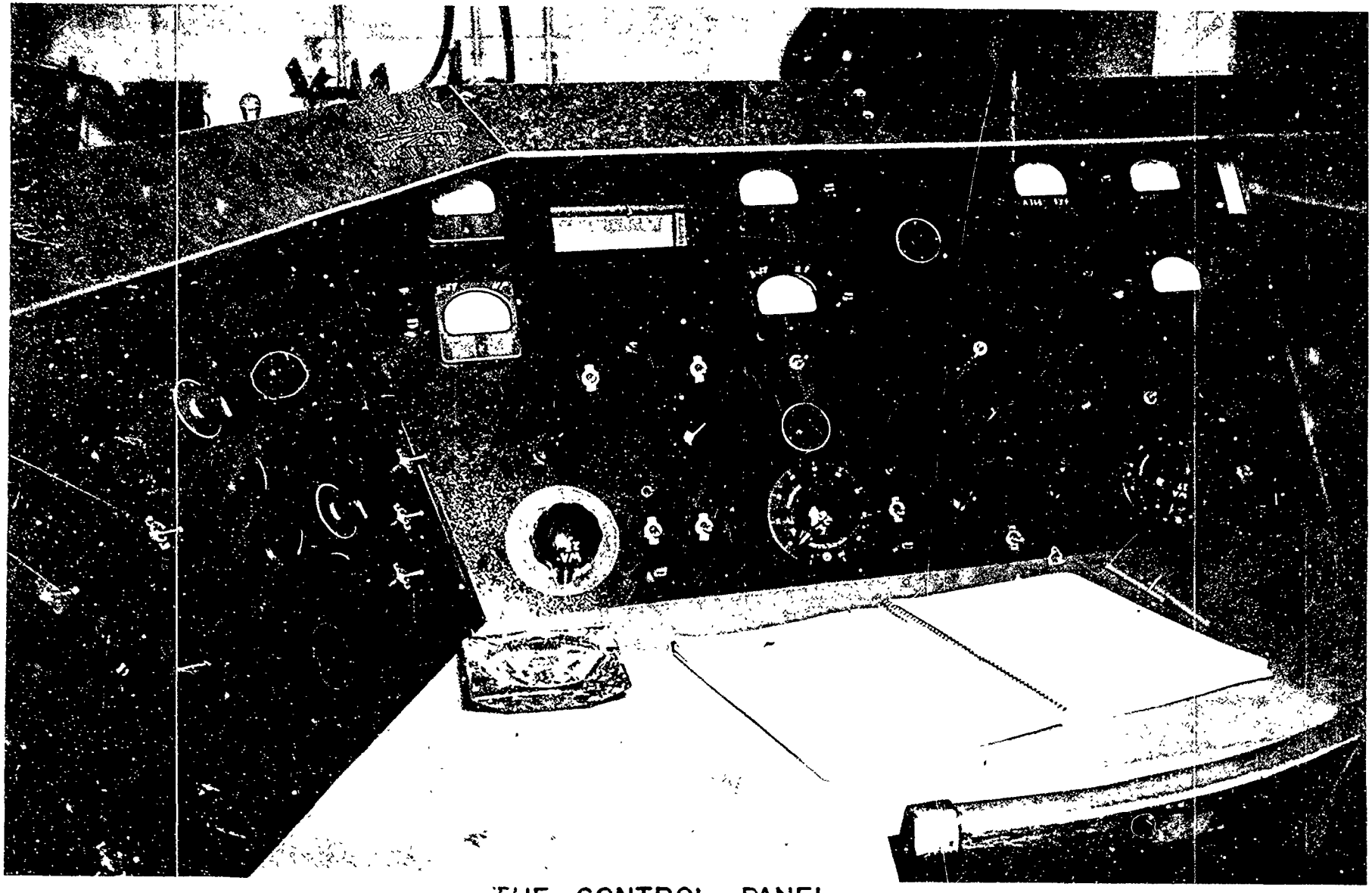

THE CONTROL PANEL

BIBLIOGRAPHY

1. Richtmyer and Kennard, Introduction to Modern Physics, pp. 245-247, McGraw-Hill Book Company, Inc., New York, 1947.

2. Davisson and Germer, "Diffraction of Electrons by a Crystal of Nickel", Physical Review 30, pp. 705-740 (1927)

3. H. E. Farnsworth, "Penetration of Low Speed Diffracted Electrons", Physical Review 49, pp. 605-609 (1936).

4. R. E. Schlier, "The Adsorption of Gases on the (100) Faces of Copper and Nickel Single Crystals using Low Speed Electron Diffraction", Doctoral Dissertation (unpublished), Brown University, 1953.

5. Handbook of Chemistry and Physics, p. 2017, 30th Edition, Chemical Rubber Publishing Company, Cleveland, 1948.

6. Davey, Study of Crystal Structure and its Applications, p. 129, McGraw-Hill Book Company, Inc., New York, 1934.

7. C. S. Barrett, Structure of Metals, p. 514, McGraw-Hill Book Company, Inc. New York, 1943.

8. Gulbransen and Andrew, "The Kinetics of the Reaction of Titanium with Hydrogen, Oxygen, and Nitrogen", The Journal of Metals 1, Number 10, Transactions p. 741 (1949).

9. R. T. Bayard and D. Alpert, "Extension of the Low Pressure Range of the Ionization Gauge", The Review of Scientific Instruments 21, p. 571 (1950).

10. H. E. Farnsworth, "A Simple Contamination-Free Electron Gun", The Review of Scientific Instruments 21, p. 102 (1950).

11. P. A. Anderson, "Contact Difference of Potential between Tungsten and Barium. The External Work Function of Barium", Physical Review 47, p. 958 (1935).

DISTRIBUTION LIST

40	Office of Ordnance Research 2 2127 Myrtle Drive Duke Station Durham, North Carolina
10	Commanding Officer Watertown Arsenal Watertown 72, Massachusetts
5	Director, Armed Services Technical Information Agency Document Services Center U. B. Building Dayton 2, Ohio ATTENTION: DSC-SD
2	Contracting Officer Boston Ordnance District Army Base, Boston 10, Massachusetts